



ELSEVIER

Tectonophysics 312 (1999) 1–33

TECTONOPHYSICS

www.elsevier.com/locate/tecto

The mechanism of ascent and emplacement of granite magma during transpression: a syntectonic granite paradigm

M. Brown*, G.S. Solar

Laboratory for Crustal Petrology, Department of Geology, University of Maryland, College Park, MD 20742, USA

Received 15 October 1998; revised version received 20 February 1999; accepted 17 March 1999

Abstract

We propose a model for syntectonic ascent and emplacement of granite magma based on structural relations in part of the northern Appalachians. In the study area in western Maine, strain was distributed heterogeneously during Devonian Acadian transpression. Metasedimentary rocks (migmatites at high grades) record two contrasting types of finite strain in zones that alternate across strike. Rocks in both types of zones have a penetrative, moderately-to-steeply NE-plunging mineral elongation lineation defined by bladed muscovite (fibrolite/sillimanite at high grades). In 'straight' belts of enhanced deformation rocks have $S > L$ fabrics that record apparent flattening-to-plane strain (apparent flattening zones, AFZs), but rocks between these belts have $L > S$ fabrics that record apparent constriction (apparent constriction zones, ACZs). At metamorphic grades above the contemporary solidus, rocks in AFZs developed stromatic structure in migmatite, which suggests that percolative flow of melt occurred along the evolving flattening fabric. Stromatic migmatites are intruded by concordant to weakly discordant, m-scale composite sheet-like bodies of granite to suggest magma transport in planar conduits through the AFZ rocks. Inhomogeneous migmatite is found in the intervening ACZs, which suggests migration of partially molten material through these zones *en masse*, probably by melt-assisted granular flow. Inhomogeneous migmatites are intruded by irregular m-scale bodies of granite that vary from elongate to sub-circular in plan view and seem cylindrical in three dimensions. These bodies apparently plunge to the northeast, parallel to the regional mineral elongation lineation, to suggest magma transport in pipe-like conduits through the ACZ rocks. We postulate that the form of magma ascent conduits was deformation-controlled, and was governed by the contemporaneous strain partitioning. Magma ascent in planar and pipe-like conduits through migmatites is possible because oblique translation during contraction displaces isotherms upward in the orogenic crust to form a thermal antiform. Within this hot corridor, it is the difference in temperature between melt-producing reactions in the anatectic zone and the wet solidus for granite melt that enables magma to migrate pervasively up through the orogenic crust without congealing. Heat advected with the migrating melt promotes amplification of the thermal antiform in a feedback relation that extends the zone of plastic deformation and pervasive melt migration to shallower levels in the crust. At the wet solidus, we suggest melt flows obliquely toward axial culminations in the thermal antiform, which are sites of melt accumulation and perturbations from which magma may escape to form plutons. Batches of melt that escape from these perturbations may be trapped by tectonic structures higher in the crust, or ascent may become inhibited with decreasing depth by thermal arrest and solidification. If the rate of arrival of subsequent melt batches exceeds the rate of crystallization at the site of pluton construction, melt pressure ultimately may lead to (sub-)horizontal magma fracture, or viscous flow of wall rocks may allow lateral spreading. The resultant plutons have (sub-)horizontal tabular geometries with floors that slope down to the

* Corresponding author. Tel.: +1-301-405-4080; Fax: +1-301-314-9661; E-mail: mbrown@geol.umd.edu

ascent conduit. As the thermal antiform decays, the height of sub-solidus crust that separates the deepest part of the pluton from the anatectic zone increases. Consequently, pluton inflation declines and solidification leads to infilling of the magma feeder channel to form a root zone that passes downward into migmatite, which may explain the difficulty of determining precisely the floor to these deeper segments of large plutons using gravimetry. © 1999 Elsevier Science B.V. All rights reserved.

Keywords: granite ascent; granite emplacement; melt flow; migmatite; pluton construction; transpressive orogen

1. Introduction

In many orogens, precise geochronology has confirmed the synchronicity implied by a spatial association between regional tectonic structures, high-grade metamorphic rocks and granites, from m-scale bodies to km-scale plutons. This spatial and temporal association suggests that granite generation, ascent and emplacement are syntectonic processes that are a fundamental feature of orogenesis (Rushmer et al., 1998). The syntectonic granite paradigm (Karlstrom, 1989) has promoted renewed debate concerning the mechanisms of ascent of granite magma through the crust (e.g., Clemens and Mawer, 1992; Brown et al., 1995a; Bittner and Schmeling, 1995; Petford, 1996; Weinberg, 1996, 1999; Paterson and Miller, 1998; Brown and Solar, 1998b), particularly through partially molten crust where evidence of how melt migrates is preserved in migmatites (e.g., Brown, 1994; Sawyer, 1994; Rutter and Neumann, 1995; Brown et al., 1995b; Collins and Sawyer, 1996; Brown and Rushmer, 1997).

Ascent is commonly described by reference to one of the two competing end-member models (e.g., Rubin, 1993) of diapirism, where the surrounding rocks deform by viscous flow (e.g., Mahon et al., 1988; Weinberg and Podladchikov, 1994), and diking, where the surrounding rocks deform elastically (e.g., Lister and Kerr, 1991). Crustal diapirism, however, is restricted to the lower part of the crust because the exponential increase in viscosity with decreasing depth in the crust stops diapiric ascent (e.g., Weinberg and Podladchikov, 1995; Vigneresse, 1995b; Bittner and Schmeling, 1995). This has led to the formulation of a composite diapir-dike model (e.g., Weinberg, 1996). Although strong geological evidence for crustal diapirism generally is lacking (e.g., Clemens et al., 1997; Clemens, 1998), recently Collins et al. (1998) have made a case for partial

convective overturn of a predominantly solid, but thermally softened crust with limited melting, and Paterson and Miller (1998) have argued for a diapiric rise of magma sheets through viscoelastic host rock during contractional deformation in continental arcs. Diking is not restricted to the lower crust, but diking *sensu stricto* refers to magma ascent by flow through a propagating fracture in elastic rock, typically in the plane perpendicular to σ_3 (e.g., Emerman and Marrett, 1990; Lister and Kerr, 1991; Rubin, 1995, 1998). Thus, diking is inhibited during regional contraction. Furthermore, although basalt dikes are ubiquitous in the crust, granite found in dikes is small in volume compared to that found in plutons. For these reasons, we do not believe that either diapirism or diking *sensu stricto* can be an appropriate general mechanism for syntectonic ascent of granite magma during transpression.

In transpressive orogens, features observed in migmatites suggest that syntectonic magma ascent occurred in conduits controlled by the tectonic structure (Brown and Solar, 1998a,b). Leucosome in migmatites, which is widely interpreted to record the former presence of some melt, even where the leucosome itself is composed of mostly peritectic or cumulate solids (Brown et al., 1995a; Sawyer, 1999), commonly is in structurally controlled sites suggesting that melt segregates in response to local pressure gradients within a deforming anisotropic source (e.g., Brown, 1994; Sawyer, 1994; Brown and Rushmer, 1997; Rutter, 1997). These observations have led to the development of pervasive flow models for melt migration within partially molten crust (e.g., Collins and Sawyer, 1996; Brown and Rushmer, 1997; Brown and Solar, 1998b; Weinberg and Searle, 1998; Vanderhaeghe, 1999). Feedback relations between deformation and melting move the solidus upward in the crust extending the zone of pervasive flow (Brown and Solar, 1998a; Weinberg, 1999).

The solidus is essentially an isotherm in the middle crust where melt porosity is occluded, which will arrest pervasive melt flow. Melt transport across the solidus may occur due to melt-enhanced embrittlement that enables fracture (Davidson et al., 1994; Brown and Solar, 1998b) or due to expulsion by elastic shock (Connolly and Podladchikov, 1998). Both mechanisms are likely to result in ascent of melt in planar conduits as sheet-like bodies or dikes *sensu lato*, the orientation of which may be controlled by mechanical anisotropy in crustal rocks (Wickham, 1987; Clemens and Mawer, 1992; Lucas and St. Onge, 1995; Brown and Solar, 1998b). Alternatively, Paterson and Miller (1998) have argued, based on experiments by Saffman and Taylor (1958) and Whitehead and Helfrich (1991), that magma fingers might form due to amplification of instabilities along an interface between two viscous fluids where movement of the fluid is perpendicular to the interface, here the solidus. Sheet-like protrusions may result from flow instabilities in circumstances where preexisting rigid boundaries exist and/or regional deformation occurs during development of the instability (Talbot et al., 1991).

With respect to the emplacement of plutons, major tectonic structures may play an important role by creating dilational space (e.g., Guineberteau et al., 1987; Hutton, 1988, 1990; Glazner, 1991; D'Lemos et al., 1992; Tikoff and Teyssier, 1992; Grocott et al., 1994), arresting ascent (e.g., Clemens and Mawer, 1992; Hogan and Gilbert, 1995; Roman-Berdiel et al., 1995; Skarmeta and Castelli, 1997), or controlling the geometry of plutons (Ingram and Hutton, 1994; Holdsworth et al., 1999; Klepeis and Crawford, 1999), although sometimes the reason for proximity between major tectonic structures and plutons is cryptic (e.g., Vigneresse, 1988, 1995a). In many circumstances magma creates some of the space required for emplacement. Thus, ballooning may cause viscous flow of the wall rocks (e.g., Cloos, 1925; Holder, 1979; Marsh, 1982; Ramsay, 1989; Guglielmo, 1993), and lateral spreading (e.g., Cruden, 1998) or vertical translation (e.g., Bateman, 1984; Cruden, 1988; Paterson et al., 1996; Morgan et al., 1998) may be accommodated by viscous flow or multiple magma transfer processes (Paterson and Fowler, 1993; Paterson et al., 1996; Hutton, 1996), including stopping at all scales (e.g., Marsh,

1982; Oxburgh and McRae, 1984; Miller and Tuach, 1989).

The role of deformation is illustrated by the Bergell pluton, Central Alps, where regional deformation contributed to final emplacement of the pluton when shortening at the base of the magma body caused an expansion at a higher crustal level and ballooning of the pluton (Rosenberg et al., 1995; Berger et al., 1996). Redistribution of mass vertically within the lithosphere is important, and lifting the country rocks above the pluton roof may occur at greater depths than previously thought, particularly in transpressive orogens (Benn et al., 1998, 1999). Broadly distributed deformation of low strain magnitude may enable emplacement and inflation of tabular plutons by depression of the pluton floor (e.g., Cruden, 1998), and both lifting of the roof and depression of the floor may contribute to accommodate the strain associated with emplacement (e.g., Grocott et al., 1999). Thus, for each pluton the space problem is solved differently, using a set of inter-linked processes and feedback relations that operate both locally and regionally.

This paper is one of a series that addresses feedback relations between deformational and thermal processes (Brown and Solar, 1998a; Solar et al., 1998; Solar and Brown, 1999a), the mechanisms of granite ascent and emplacement (Brown and Solar, 1998b), and the internal structure and composition of individual plutons (Brown and Pressley, 1999; Pressley and Brown, 1999) in transpressive orogens. These issues are important because the large number of plutons present in contractional orogenic belts, and the close spacing between them, implies a significant contribution from pluton emplacement dynamics to regional orogenic deformation and a significant mass exchange between the lower and upper crust. To understand better the feedback relations that operate during orogenesis, it is necessary to document examples in which development of regional tectonic structures, metamorphism and ascent of granite magma are shown to be synchronous. Our area of study is in western Maine–eastern New Hampshire, in the northern part of the Appalachian orogen of eastern North America (Fig. 1). Here, U–Pb monazite and zircon crystallization ages of granites (Solar et al., 1998) and microstructural relations in metamorphic rocks of the Central Maine belt

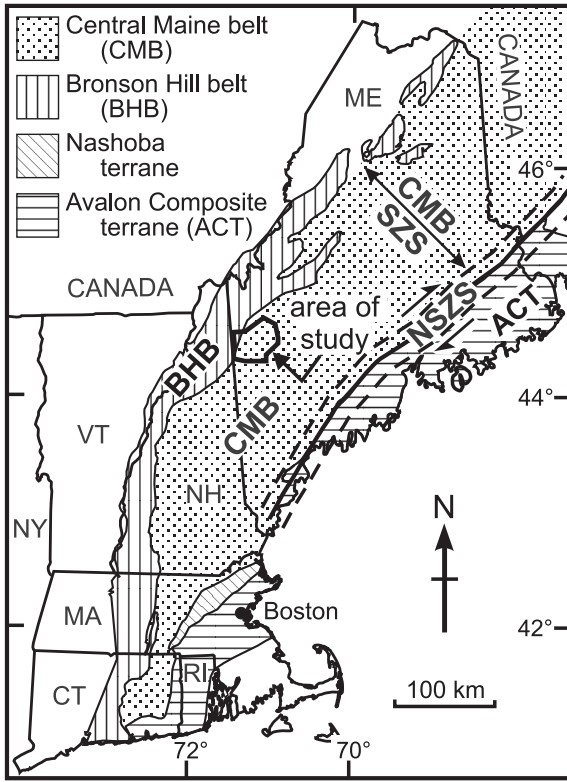


Fig. 1. Location map of area of study in western Maine, within the northern Appalachian orogen of eastern North America. CMBSZS = Central Maine belt shear zone system; NSZS = Norumbega shear zone system; ME = Maine; NY = New York; VT = Vermont; NH = New Hampshire; MA = Massachusetts; CT = Connecticut; RI = Rhode Island.

(Solar and Brown, 1999a) support synchronous deformation, metamorphism and emplacement of granites. In this paper, we describe the relations between: (1) a crustal-scale shear zone system with alter-

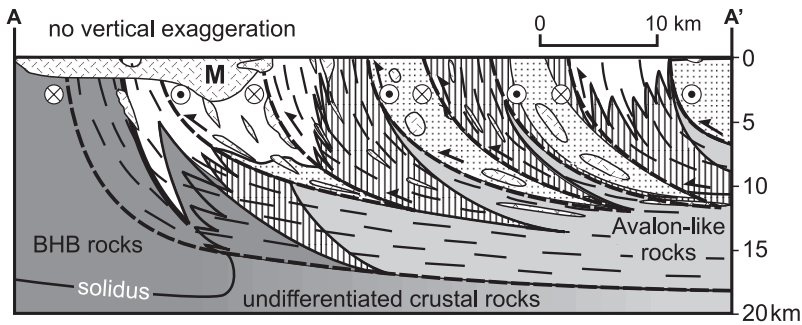
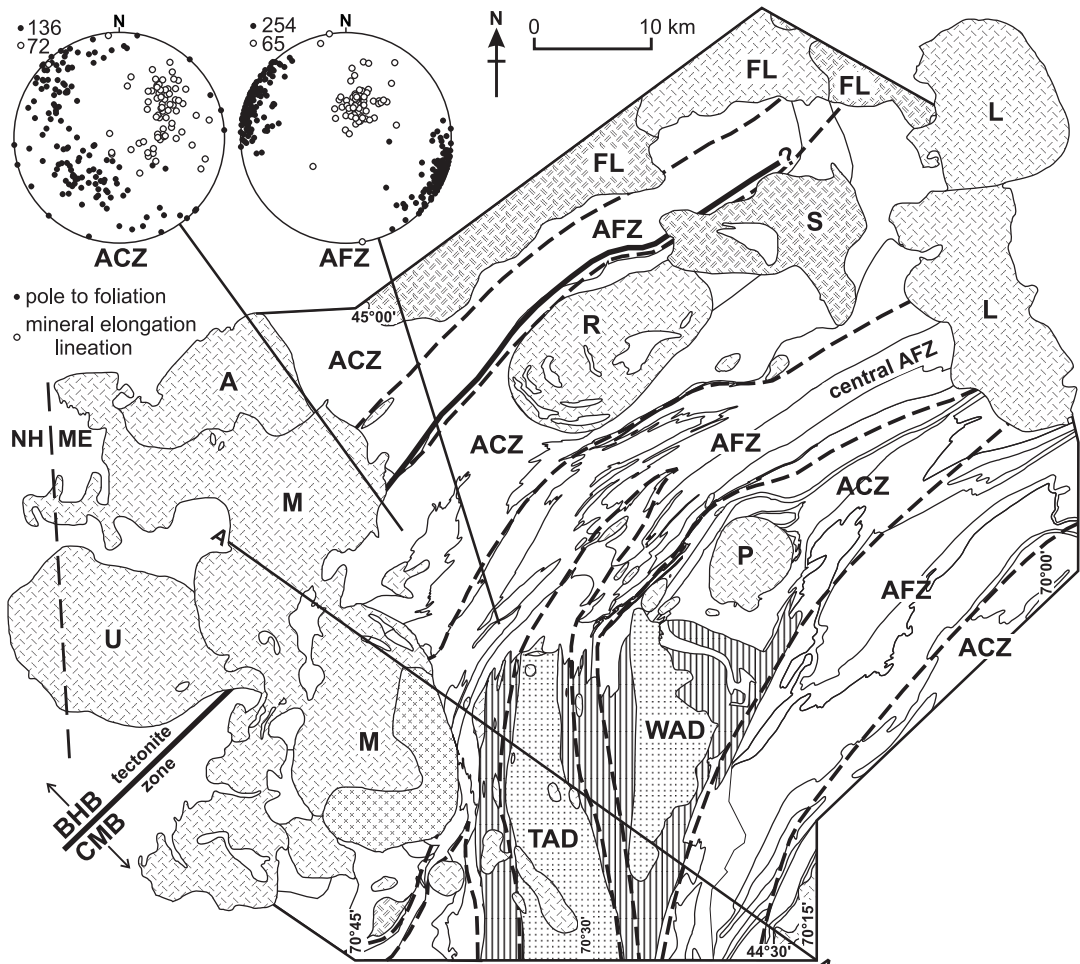
nating zones of contrasting patterns of finite strain that reflect partitioning of flow during oblique contractional deformation; (2) different structural types of leucosome in migmatite and small-scale bodies of granite found in the migmatites that have forms varying from stromatic and sheet-like to rod-shaped and cylindrical, which we interpret to represent melt-escape structures; and (3) granite plutons, which represent sinks for melt extracted from the anatectic zone. Based on this example, we propose a general model for syntectonic ascent and emplacement of granite magma that may be applicable to other transpressive orogens.








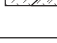


2. Regional geology of western Maine–eastern New Hampshire, northern Appalachians, USA

In the northern Appalachians, Paleozoic rocks have been divided into several tectonostratigraphic belts (Fig. 1). The area of study is within the Central Maine belt (CMB), which is a NE-trending belt of greenschist to upper amphibolite facies metasedimentary rocks and plutonic complexes. To the northwest (Fig. 1) are Ordovician metasedimentary and metavolcanic rocks of the Bronson Hill belt (BHB), which were deformed and metamorphosed during the Ordovician Taconian orogeny (Ratcliffe et al., 1998, and references therein). To the southeast (Fig. 1), the CMB is truncated by the Norumbega shear zone system (NSZS), along which the Neoproterozoic to Silurian Avalon Composite Terrane was juxtaposed against the CMB during the Silurian–Early Devonian (West and Hubbard, 1997; West, 1999).

In the CMB of western Maine and eastern New Hampshire, metamorphic grade increases along

Fig. 2. Simplified geological map of a portion of western Maine and adjacent New Hampshire, USA. The Siluro-Devonian stratigraphy is unornamented, separated by solid lines. Field data (Solar, 1996; Brown and Solar, 1998a; Solar and Brown, 1999b) supported by microstructural observations (Solar and Brown, 1999a,b) allow distinction between ‘straight’ belts of enhanced deformation that record apparent flattening-to-plane strain, and higher strain (AFZ), and areas of more variable attitude of structures that record apparent constrictional strain, and lower strain (ACZ). Representative stereograms (lower hemisphere, Schmidt projections) of poles to foliations (dots) and lineations (circles) for one domain in an example of an ACZ and an AFZ are shown to illustrate the difference in structural style. Stereograms are part of a larger data set in Solar and Brown (1999b). The structure section along the line A–A’ is shown without vertical exaggeration. Based on available geological and geophysical data (discussed in the text), the overall geometry of the CMBSZS is listric, shallowing to a sub-horizontal root zone at ~13 km depth. The Avalon-like rocks beneath the CMB rocks are inferred based on geophysical and geochemical arguments (discussed in the text). The position of the solidus at depth is inferred on the basis of geological reasoning, using information such as the change in metamorphic grade at the surface.



- | | |
|---|--|
|  Tumbledown and Weld Anatexic Domains (TAD and WAD; stromatic/inhomogeneous migmatite) |  Redington pluton (biotite granite) |
|  Adamstown pluton (granite - monzodiorite) |  Sugarloaf pluton (diorite - granodiorite) |
|  Flagstaff Lake igneous complex (gabbro/biotite granite) |  Umbagog pluton (biotite granite) |
|  Lexington pluton (biotite granite - leucogranite) |  smaller bodies of leucogranite, granodiorite, pegmatite/gabbro |
|  Mooselookmeguntic pluton (leucogranite/granodiorite) | — stratigraphic contact |
|  Phillips pluton (leucogranite, granodiorite) | - - - boundary of structural zone |

strike to the southwest (Guidotti, 1989), from biotite zone conditions to upper sillimanite zone conditions. At the highest metamorphic grades, in the Tumbledown and Weld anatectic domains of the study area (TAD and WAD, Fig. 2) and to the southwest in New Hampshire (Moench et al., 1995), the metamorphic rocks are migmatitic, which we interpret to reflect conditions above the contemporary solidus. The main penetrative deformation and metamorphism recorded within the CMB rocks, and the associated plutonism, are the result of Devonian Acadian orogenesis (Eusden and Barreiro, 1988; Smith and Barreiro, 1990; Bradley et al., 1998; Solar et al., 1998, and references therein). The Acadian orogeny of the northern Appalachians was transpressive (van der Pluijm and van Staal, 1988; Swanson, 1992; de Roo and van Staal, 1994; van Staal and de Roo, 1995; van Staal et al., 1998). Thus, strain was partitioned between oblique contraction across the Central Maine belt shear zone system (CMBSZS; Brown and Solar, 1998a,b; Solar and Brown, 1999a,b) and dextral-transcurrent displacement along the NSZS (West and Hubbard, 1997; West, 1999).

Regional mapping and analysis of mesoscopic and microscopic structures show that strain was distributed heterogeneously in the CMB of western Maine, with rocks recording two contrasting types of finite strain in zones that alternate across strike to define the CMBSZS (Solar and Brown, 1999a,b). Metasedimentary rocks in both types of zones have a penetrative, moderately-to-steeply NE-plunging mineral elongation lineation defined by bladed muscovite (Fig. 2, stereograms). 'Straight' belts are characterized by tight folds of the stratigraphic succession, a strongly developed and consistently oriented foliation, sub-parallel strike-of-foliation form lines, and $S > L$ fabrics (Brown and Solar, 1998a; Solar and Brown, 1999a,b). In contrast, the intervening zones between 'straight' belts are characterized by open folds of the stratigraphic succession, a weakly defined, variably oriented foliation, and $L > S$ fabrics (Brown and Solar, 1998a; Solar and Brown, 1999a,b). A variety of mesoscopic asymmetric structures in 'straight' belt rocks show dextral-SE-side-up kinematics in response to the oblique contraction (Solar and Brown, 1999b).

The tectonic fabrics in both types of zones are defined by the same minerals at the same metamor-

phic grade, with bladed muscovite being replaced as a fabric-forming mineral by fibrolite/sillimanite at the highest metamorphic grades, so that the accommodation of strain and metamorphic recrystallization are interpreted to have occurred together across the CMBSZS (Solar and Brown, 1999a). Biotite 'fish' and quartz-dominated polycrystalline aggregates in asymmetric strain shadows around porphyroblasts, which are elongate in the mineral elongation direction, show consistent dextral-SE-side-up displacement along the mineral elongation lineation in the plane of the foliation. Porphyroblasts of andalusite and staurolite in both types of zones have preferred orientations, statistically parallel to matrix fabrics (Solar and Brown, 1999a). In 'straight' belt rocks, porphyroblasts of garnet and staurolite include foliation that is discontinuous with matrix foliation. In contrast, inclusions in porphyroblasts in the intervening zone rocks do not show a preferred orientation fabric. The obliquity between inclusion trails in garnet and staurolite and the surrounding matrix fabric in 'straight' belt rocks records tightening of folds and reorientation of matrix fabrics with respect to porphyroblasts as flattening strain was accommodated preferentially in these zones (Solar and Brown, 1999a,b).

The mineral fabrics are interpreted to record the tectonic strain ellipsoid. Thus, rocks in 'straight' belts record apparent flattening-to-plane strain and qualitatively higher strain than rocks in the intervening zones, which record apparent constriction strain and qualitatively lower strain. We call these zones of apparent flattening (AFZ) and zones of apparent constriction (ACZ), respectively. Thus, finite strain in the study area shows a spatial variation in type and magnitude that reflects kinematic partitioning of flow in the CMBSZS, likely a product of concentration of strain at thrust-ramp anticlines (Solar and Brown, 1999b). As the system evolved, the orogenic front migrated inboard as successive thrust-ramp anticlines formed during serial development of folding instabilities, and flattening strain became concentrated at each of these structures to partition the flow.

Peraluminous granites derived from a Central Maine belt source suggest that part of the progressively thickening stratigraphic succession exceeded the solidus temperature for mica dehydration melting

(Pressley and Brown, 1999). This partially molten crust likely formed the décollement layer in which the CMBSZS is rooted (Solar and Brown, 1999b). The décollement layer is inferred to lie immediately above the contact between CMB rocks and the underlying basement. Based on interpretations of geophysical data (Stewart, 1989; Zhu and Ebel, 1994; Musacchio et al., 1997), supported by geochemical arguments (Pressley and Brown, 1999), the basement is interpreted to be similar to the Neoproterozoic gneisses and plutons of the Avalon Composite Terrane. We call this unexposed basement, which forms part of Avalonia as defined by Cocks et al. (1997), Avalon-like crust. This is consistent with the view of Stewart (1989), based on a review of the geophysical data collected over the past fifteen years, that the “... low-velocity deepest crust and lithosphere likely is peri-Gondwanan Silurian composite terrane that was thrust under rocks of the Central Maine (belt) during the Acadian orogeny.”

3. Migmatites in west-central Maine

Displacement accommodated by the CMBSZS was dextral-SE-side-up, so that blocks on the southeast side were obliquely thrust inboard to the northwest and along strike to the southwest. Thus, the block to the southeast of the central AFZ exposes a deeper structural level than the block to the northwest, from the central AFZ to the Greenvale Cove

tectonite zone (Fig. 2), consistent with available thermobarometric data (see below and in Brown and Solar, 1998b). The Weld and Tumbledown anatectic domains (WAD and TAD) form part of the deeper structural level within the area of study (see structure section in Fig. 2).

Migmatitic rocks are restricted to the WAD and TAD (Fig. 2), which have sharp contacts with non-migmatitic rocks. The locus of points representing the first appearance of migmatite in an upgrade direction along the metamorphic field gradient is the ‘migmatite front’ or migmatite-in isograd (Fig. 2), which corresponds to the intersection with Earth’s surface of the isograd surface in three dimensions. This isograd records the wet solidus for granite melt. A section along the line A–A’ (Fig. 2) through this surface is shown in Fig. 3 in a projection view northeast down-plunge of the mineral elongation lineation. Making the assumption that the ‘migmatite front’ is approximately isothermal (discussed below), the three-dimensional form of this front reflects the thermal structure of the orogen, which is antiformal, consistent with the results of modeling (cf. Huerta et al., 1996, 1998, 1999; Thompson et al., 1997; Jamieson et al., 1998).

Within the WAD and TAD, migmatites have been divided into stromatic and inhomogeneous structural types (Solar, 1996; Brown and Solar, 1998a,b). We use the term inhomogeneous migmatite for rocks that do not preserve a regular mesosome–melanosome–leucosome layered structure. The spatial distribution

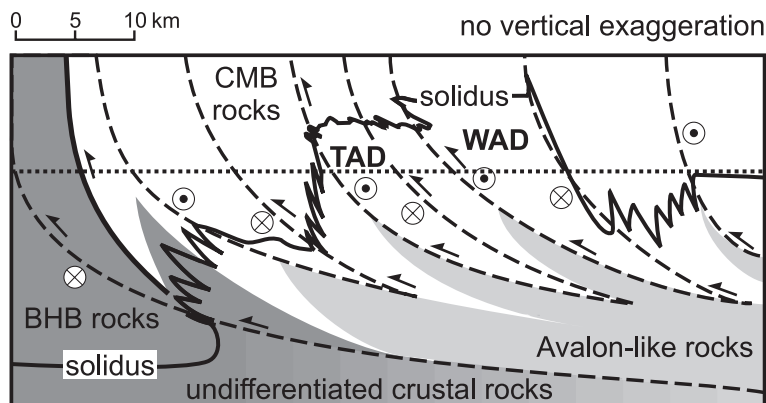


Fig. 3. Projection down-plunge of the mineral elongation lineation to show the form of the solidus as represented by the ‘migmatite front’ around the Tumbledown and Weld anatectic domains (TAD and WAD), western Maine, USA. The projection is drawn along the line of section AA’ shown in Fig. 2. The short-dash line represents the intersection of the map plane with the plane of the projection; CMB = Central Maine belt; BHB = Bronson Hill belt.

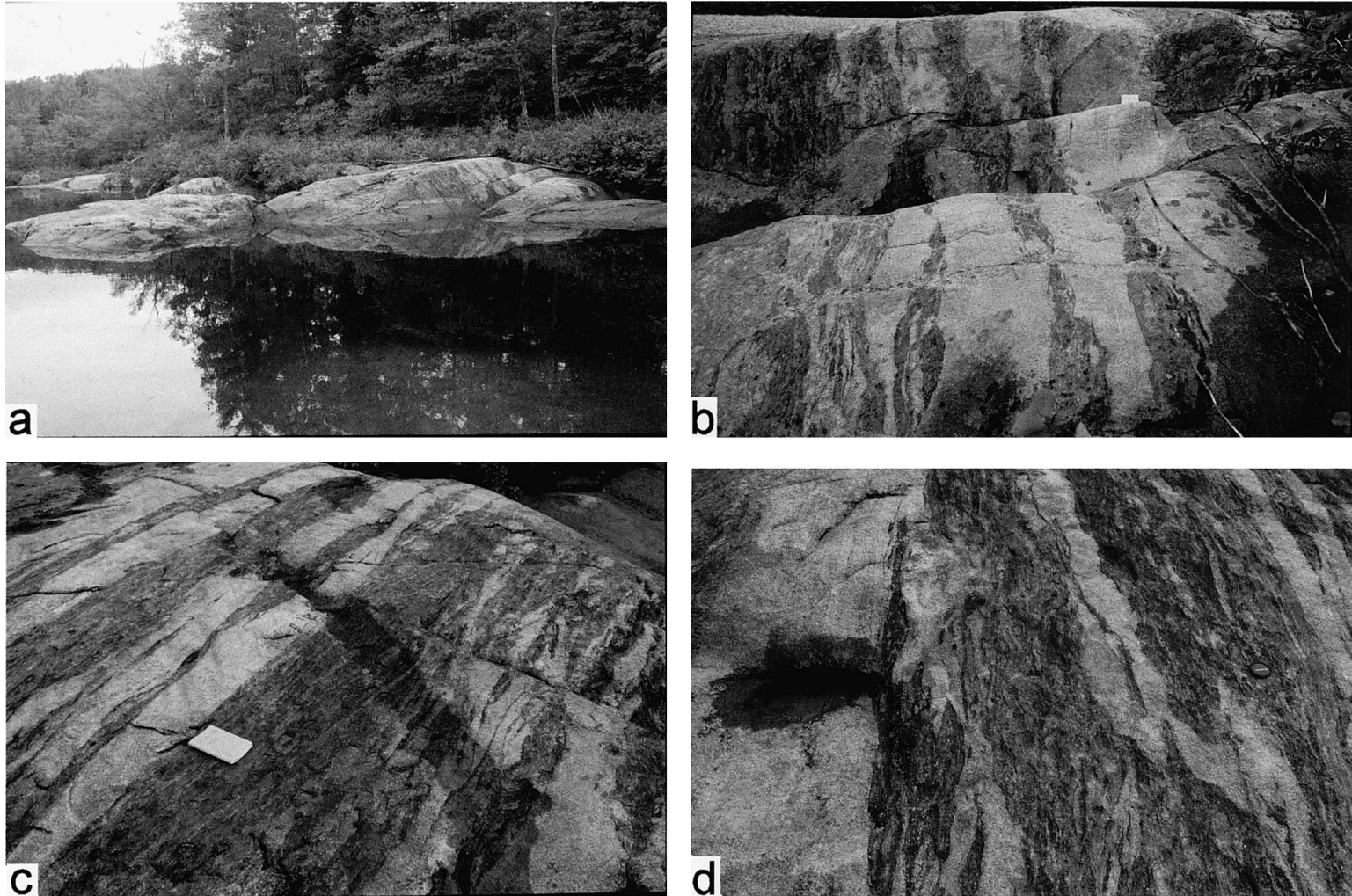


Fig. 4. (a) View to the northeast of low outcrop of stromatic migmatite with sheet-like bodies of granite within the central AFZ, Swift River, Roxbury, west-central Maine, USA. (b) Oblique view to the north-northeast of the steeper southern end of outcrop shown in (a). (c) View to the southeast across sub-horizontal top surface of the outcrop to show in more detail the stromatic migmatite and steeply east-dipping sheet-like bodies of granite. Note that the sheet-like bodies of granite to the western (lower) side of the outcrop are more irregular in form, whereas those to the eastern (upper) side of the outcrop are essentially planar. (d) Closer view of top surface of outcrop to show details of stromatic migmatite structure, discordant sheet-like bodies of granite with pinch-and-swell structure, and the magmatic fabric in the thicker, composite planar granite sheet on the left-hand side of the field of view (shown in detail in Fig. 5).

of these different migmatite types correlates with the major structural zones distinguished on the basis of different apparent tectonic strain ellipsoids recorded by the fabrics (Solar and Brown, 1999a,b). Stromatic migmatite is found in the AFZs, although it occurs marginally to the AFZs in the ACZs (Fig. 2). Inhomogeneous migmatite is restricted to the ACZs (Fig. 2). As the CMB shear zone system crosses western Maine from northeast to south (Fig. 2), planar structures in the AFZs change in strike, and linear structures change in trend, from NE–SW to N–S from across the area (Brown and Solar, 1998b; Solar and Brown, 1999b), and revert to NE–SW farther southwest outside the area of study (Moench et al., 1995). Concurrently, lineations vary from moderately plunging to steeply plunging and back to moderately plunging. This geometry and the asymmetric map patterns of the ACZs suggest that the CMBSZS in west-central Maine forms a restraining bend within a regional-scale dextral-SE-side-up structure. The inhomogeneous migmatites are concentrated within the asymmetric ACZs in the region of this bend.

3.1. Melt-escape structures in stromatic migmatite

The migmatite leucosomes in stromatic migmatites are (sub-)parallel to the fabric in the host rock (Fig. 4), which commonly has residual mineralogy. Although the leucosomes are likely to be locally derived, they may represent melt or some crystalline product (residual, peritectic or cumulate phases) trapped during syntectonic migration parallel to the fabric, rather than stagnant melt crystallized in situ (cf. Brown et al., 1995a,b; Brown and Brown, 1997). The leucosomes have higher aspect ratios in sections approximately parallel to lineation compared to sections at a high angle to lineation and an overall planar sheet-like geometry elongate along the mineral elongation lineation, consistent with continued accumulation of flattening-to-plane strain during formation.

In thin sections oriented perpendicular to foliation and parallel to mineral elongation lineation, leucosomes do not exhibit strong evidence of subsolidus plastic strain, although quartz commonly shows some grain boundary migration and sub-grain structure. K-feldspar occurs as equant to elongate

(length-to-width ratio of $\sim 2:1$) anhedral crystals (sub-)parallel to the leucosome boundaries and a magmatic biotite foliation. Equant K-feldspar, plagioclase and quartz grains have boundaries that may meet in triple junctions. Also, plagioclase occurs as strongly zoned rounded crystals, interpreted to be residual from melting, and weakly zoned crystals euhedral against quartz, interpreted to have crystallized from melt. These features suggest a predominantly magmatic microstructure.

We interpret the three-dimensional shapes of the leucosomes, and their concordance with metamorphic fabrics in the melanosomes and mesosomes, to reflect syn-anatectic strain rather than strain imposed after solidification. This means that their shape reflects both the contemporary deformation and the control on flow paths imposed by the progressively developing structures. The common coincidence of foliation and mm- to cm-scale leucosomes in stromatic migmatites (Fig. 4d) suggests percolative flow of melt along the flattening fabric using the dynamic permeability produced during active deformation (Brown and Solar, 1998b).

Concordant to weakly discordant, irregular to planar, sheet-like bodies of granite are intruded into the migmatites (Fig. 4a–c), which suggests magmatic flow in planar conduits parallel to or at a low angle to the foliation (Brown and Solar, 1998a,b). In one example, multiple m-scale sheeting at a site in the central AFZ enabled construction of a highly elongate elliptical pluton ~ 5 km long and ~ 1 km across. Commonly the larger sheets are composite, being composed of multiple cm-scale sheets of granite with small differences in grain size and/or mode and/or texture, some of which are separated by biotite-rich schlieren, to suggest pulsed flow of multiple magma batches through these channels (Fig. 4d and Fig. 5). In combination with other magmatic flow structures, such as asymmetric biotite-rich schlieren and trails of biotite crystals, these features show that granite in sheets is exotic to the outcrop.

The larger sheets of granite, which locally cut the foliation and stromatic structure at a shallow angle, are connected to the smaller, more obviously discordant sheets of granite, and these sheets sometimes are seen to be connected to the finer-scale leucosomes interlayered with melanosome in the host migmatite (Fig. 4d). This suggests that the melt

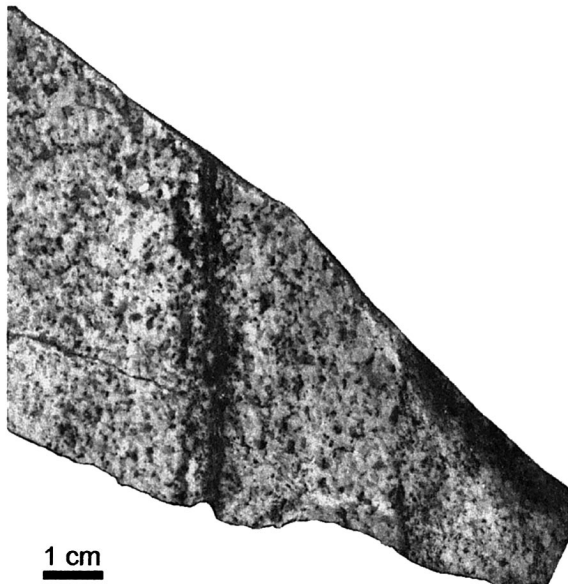


Fig. 5. Polished surface of an oriented hand sample showing a steep contact in (sub-)horizontal section between two dm-scale sheets of granite from the composite m-scale sheet shown in Fig. 4d (left). The slab face is oriented sub-normal to magmatic foliation, and north is toward the top of the diagram, consistent with Fig. 4b. The contact between the two sheets is coincident with a mm-scale biotite-rich schlieren. Granite on the eastern (right) side has a better-defined biotite foliation and finer grain size relative to granite on the left.

flow network was connected at all scales observed at outcrop. Thus, the larger-scale flow network, represented by the planar conduits, was connected to the smaller-scale storage network, represented by the migmatite leucosomes.

In detail, on both shallowly oriented and steeply oriented surfaces, the m-scale granite sheets exhibit pinch-and-swell structure (Fig. 4), although no significant solid-state deformation is recorded by the granite other than by quartz. Biotite found in flattened schlieren is interpreted to be residual from melting, but smaller individual crystals of euhedral biotite apparently crystallized from the melt. These features suggest that accumulation of plastic strain outlasted emplacement of the granite, and that some deformation occurred after final crystallization of the granite. Based on these observations, we interpret the three-dimensional form of these planar sheet-like bodies to reflect the form of the syntectonic magma flow channels through the AFZs.

3.2. Melt-escape structures in inhomogeneous migmatite

In inhomogeneous migmatites, although the vol.% leucosome is variable, commonly a qualitatively higher vol.% leucosome is present in comparison with the vol.% leucosome preserved in stromatic migmatites. This observation suggests that more melt was retained in the inhomogeneous migmatites than in the stromatic migmatites, or that melt infiltrated the ACZs pervasively, perhaps from the AFZs, or that both retention and infiltration occurred. Furthermore, leucosome–melanosome segregation is more diffuse, although leucosome concentrations are common (Fig. 6a,c), and interconnected leucosome networks are typically preserved (Fig. 6d). All gradations exist between dark inhomogeneous migmatites with a residual aspect (the melt-depleted diatexites of Sawyer, 1998) and schlieric granite (the melt-enriched diatexites or diatexite magmas of Sawyer, 1998), which suggests melt migration and redistribution within the partially molten system.

In three dimensions, the cm-scale leucosome concentrations vary from highly inequidimensional layers to rods, both of which are elongate parallel to the mineral elongation lineation recorded in the surrounding melanosome. In inhomogeneous migmatites transitional to schlieric granite, there are flow structures similar to those in granite sheets (Brown and Solar, 1998b; Fig. 4c,d), and concentrations of quartz and feldspar are present as tails at the ends of enclaves to suggest accumulation of melt, magma or crystals in areas of low pressure during flow (cf. Sawyer, 1996). Based on these observations, we infer migration of partially molten material through the ACZs both en masse by melt-assisted granular flow (at low melt-fraction, either undepleted bulk compositions with a low degree of melting, or melt-depleted diatexites) and in batches by magmatic flow of melt carrying entrained residue (at high melt fraction, melt-enriched diatexites and diatexite magmas) (cf. Bittner and Schmelting, 1995; Sawyer, 1996, 1998; Rutter, 1997; Bagdassarov and Dorfman, 1998; Petford and Koenders, 1998).

Within the inhomogeneous migmatites, granite is present as discrete, irregular m-scale low length-to-width ratio planar sheet-like (Fig. 6b) and linear cylindrical (Fig. 7) bodies. These bodies plunge sim-

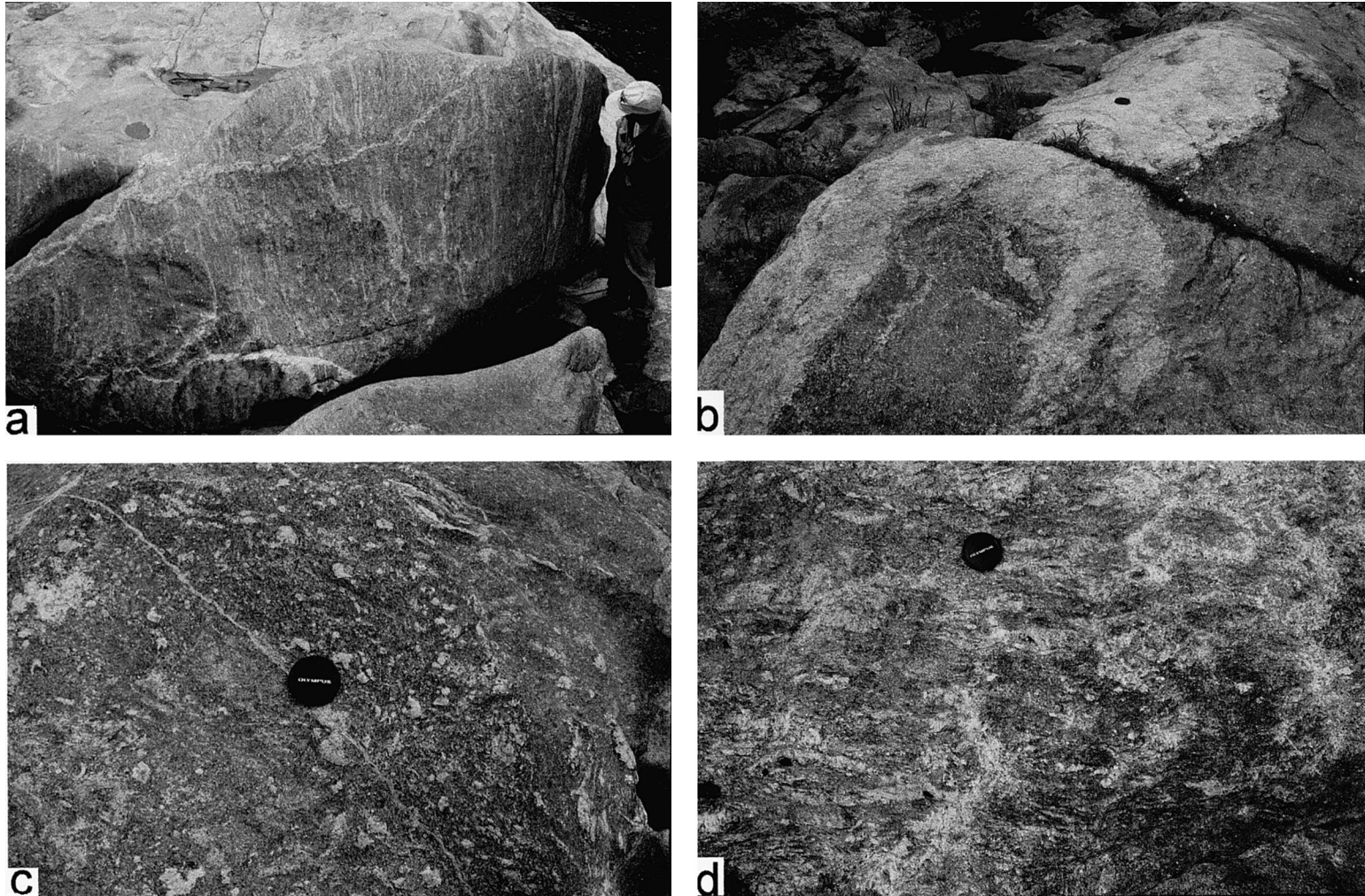


Fig. 6. (a) Foliated inhomogeneous migmatite at the transition between stromatic and inhomogeneous migmatite domains at the eastern margin of the central AFZ (view to the south); leucosome has a higher aspect ratio on steep surfaces than on shallow surfaces, which emphasizes the transition from planar leucosomes (flattening-to-plane strain) to elongate linear leucosomes (constrictional strain), Roxbury, west-central Maine, USA. (b) Melt-escape structure that has a low length-to-width ratio shape on this shallow outcrop surface to suggest a transitional sheet- or rod-shaped body, rather than the planar sheet-like bodies of Fig. 4 (view to the north), Roxbury, west-central Maine, USA. (c) Steeply inclined outcrop surface cuts through leucosome rods in inhomogeneous migmatite, Swift River, Roxbury, west-central Maine, USA. (d) Steeply inclined outcrop surface, approximately perpendicular to mineral elongation lineation, which cuts through inhomogeneous migmatite in which leucosome is connected to form a percolation network with a long axis of similar plunge to the regional mineral elongation lineation (view to the east), 50 m to the south of (c), Swift River, South Roxbury, west-central Maine, USA.

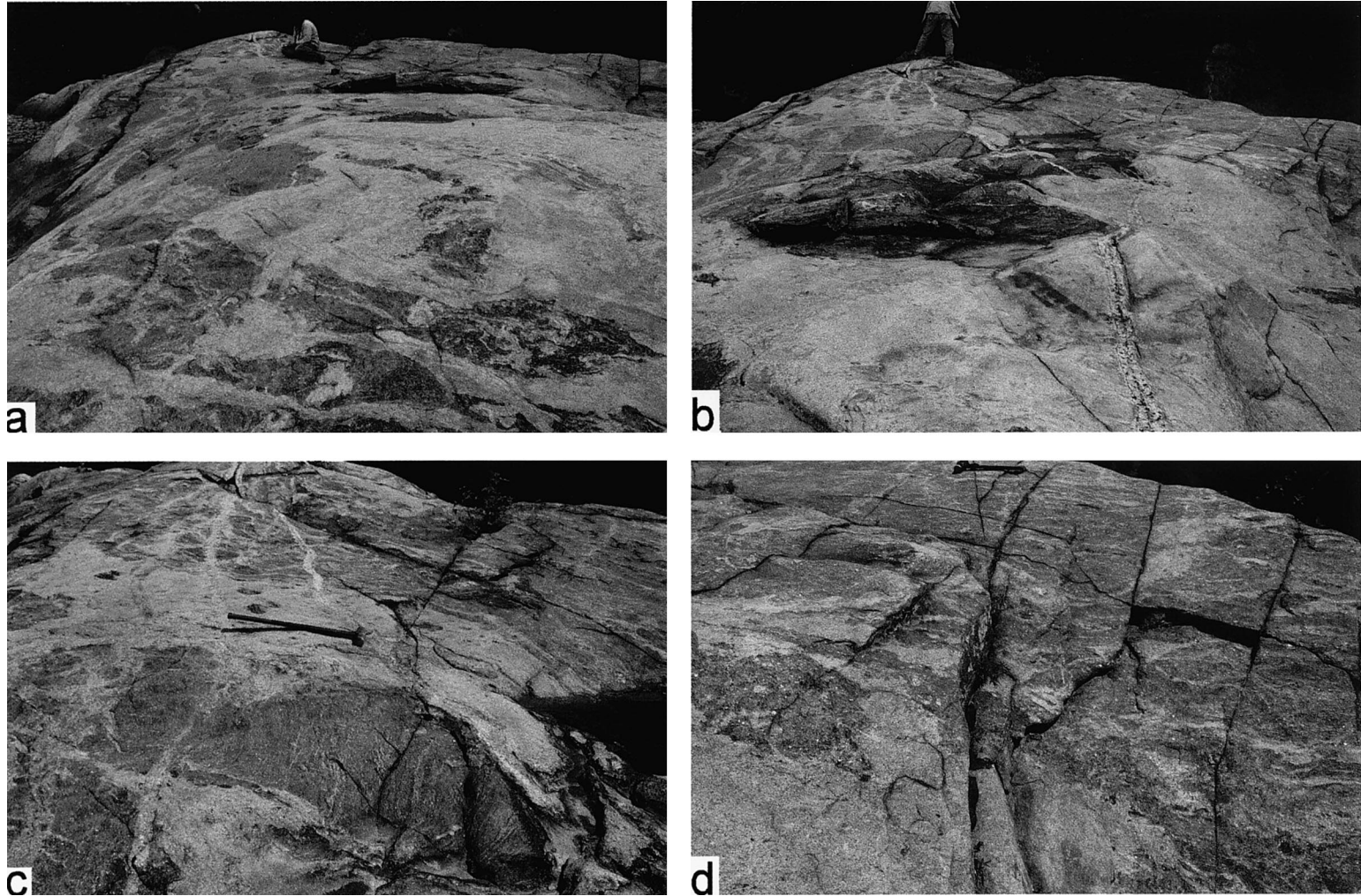


Fig. 7. Views of rod-shaped body in outcrops on the east side of the Swift River, north Roxbury, west-central Maine, USA. (a) View northeast along the northwestern margin of rod-shaped body of granite, ~10 m in diameter, to show a magmatic fabric parallel to the margin of the body and stoped and rotated blocks of locally derived veined inhomogeneous migmatite. (b) An exotic melanocratic enclave of residual material toward the center of the body, view to the northeast. (c) Magmatic foliation in granite and foliation in host inhomogeneous migmatite are parallel, but the orientation of the foliation in stoped blocks lies at a high angle to the regional trend to suggest that the blocks have been rotated, view to the northeast at northeastern margin of body. (d) View of eastern margin of body to show connected nature of granite from the rod-shaped body into the surrounding leucosome of the inhomogeneous migmatite.

ilarly to the cm-scale rod-shaped leucosome concentrations and the mineral elongation lineation in the migmatite mesosomes. In one sub-circular structure that is up to 10 m across (Fig. 7a), m-scale blocks of sillimanite–garnet–biotite-rich melanosome are present within the exposed area of (schlieric) granite (Fig. 7b). These blocks have a more residual appearance and are dissimilar to locally derived m-scale blocks of inhomogeneous migmatite that are present toward the margin of the body (Fig. 7b,c). We postulate that the granite ascended by magmatic flow as the melanosome blocks sank by particle sedimentation (e.g., Bagdassarov et al., 1996).

Granite from the main body of this structure penetrates the surrounding inhomogeneous migmatite as a vein network that connects with leucosome concentrations (Fig. 7d). This shows that this larger melt-escape structure is connected with the storage porosity represented by the smaller granite veins and leucosome pods in the surrounding migmatite. Although the three-dimensional form of this structure can be inferred only from a few meters of vertical exposure at outcrop (Fig. 7), the sub-circular plan view and apparent steeply plunging orientation suggest that it likely represents a major pipe-like magma flow conduit.

3.3. Discussion

The stromatic migmatites preserve a lower vol.% leucosome, which may imply that less melt was retained in these rocks than in the inhomogeneous migmatites, consistent with the residual nature of some stromatic migmatites implied by mineral modes of melanosomes. Many inhomogeneous migmatites, however, have a residual nature to suggest that melt has been driven out of both types of migmatites (G.S. Solar and M. Brown, unpubl. data). Melt loss from structurally deeper levels is represented by m-scale sheets of granite in the stromatic migmatites and m-scale low length-to-width ratio sheets and cylinders of granite in the inhomogeneous migmatites, both of which represent granite magma that became stuck in the conduit system.

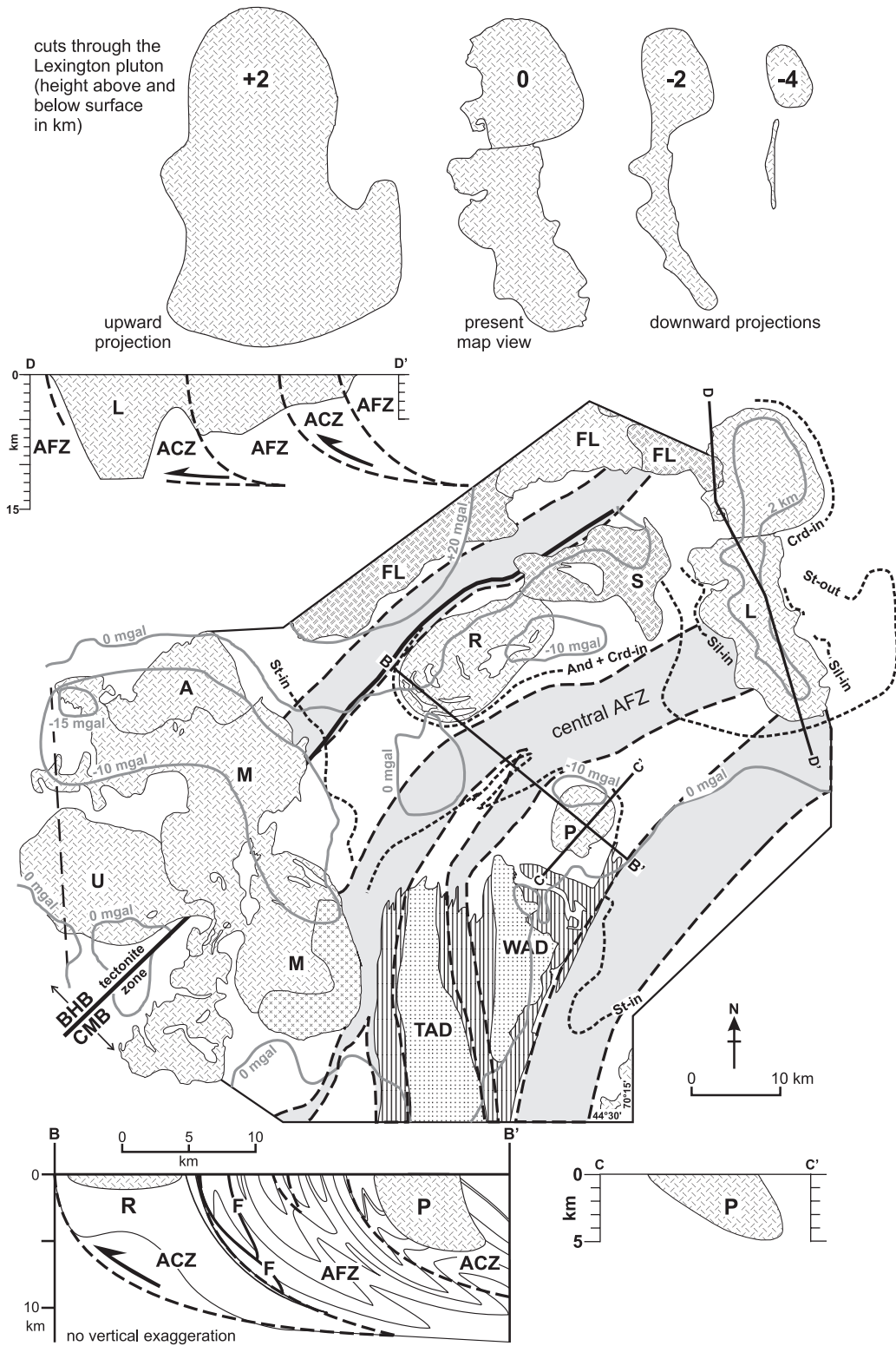
In AFZs, rocks that record apparent flattening fabrics are associated with planar bodies of granite at a variety of scales, many of which are concordant with host-rock fabrics, although some are weakly discor-

dant (Brown and Solar, 1998b). In ACZs, rocks that record apparent constriction fabrics are associated with cylindrical bodies of granite at a variety of scales. This suggests that the form of melt-escape structures was deformation-controlled, and was governed by strain partitioning. Based on these observations, we interpret the CMBSZS to represent a percolation network that focused melt flow through the crust (Brown and Solar, 1998a,b). We infer that buildup of melt pressure leads to transient change in the effective permeability of the flow network, and cyclic fluctuation of melt pressure enables escape by pulsed flow of melt through the source. The solidus surface represents the limit of syntectonic pervasive melt flow through the orogen, what may happen at this surface is discussed below.

4. Granite plutons in western Maine–eastern New Hampshire

The three-dimensional form of plutons can be deduced by combining geologic information with models based on geophysical data, in particular gravity anomalies (e.g., Vigneresse, 1988). This approach is important in poorly exposed terrain, such as the CMB in western Maine–eastern New Hampshire. In this paper, we use the pluton geometries derived by Brown and Solar (1998b). The pluton geometries they derived are speculative due to restrictions imposed by the amount of outcrop, the size of the gravity data sets, and the intrinsic limitations in modeling of residual gravity anomalies (e.g., Vigneresse, 1990). Furthermore, downward thicknesses estimated from gravity data represent minima. First, the proportion of each pluton removed by erosion cannot be deduced, except where part of the roof contact is preserved or the metamorphic imprint beneath the floor of the removed granite remains. Second, the position of the pluton floor must be uncertain in circumstances where the pluton may be gradational downward into migmatites, although a floor must be defined to model the residual gravity anomalies.

For our purpose we concentrate on two plutons, the Phillips pluton, which is within the block to the southeast of the central AFZ, and the Lexington pluton, which is within the block to the northwest of the central AFZ (Figs. 2 and 8). Given the im-



plication of the dextral-SE-side-up kinematics that successively shallower structural levels are exposed to the northwest, we use these granites to illustrate the progression from contemporaneous deeper to shallower levels across the central AFZ (Brown and Solar, 1998b).

4.1. The Phillips pluton

The Phillips pluton is composed of dominantly medium-coarse-grained two-mica leucogranite and subordinate fine-medium-grained granodiorite (Pressley and Brown, 1999). It is weakly elliptical in map view, 8 km in long dimension, parallel to regional structure, and 6 km across, and is in the ACZ to the southeast of the central AFZ (Figs. 2 and 8). Magmatic fabrics (Fig. 9a; planar biotite-rich schlieren, and modal and grain-size layering) are present locally in the leucogranite and are oriented conformably with the NE-striking foliation in the surrounding metasedimentary units, which are amphibolite facies metapelites and metapsammites. Where observed, local contacts between granite and metasedimentary rocks are concordant and NE-striking, similar to the regional structures; pluton contacts are steeply SE-dipping on the northwestern and southeastern sides of the pluton, and apparently NE-dipping on the northeastern side. In pavement outcrop within a discrete body of leucogranite on the northwest side of the pluton, the leucogranite exhibits a sheeted structure in which structurally concordant screens of pelitic schist occur, and sheets of leucogranite and pegmatitic granite occur within the pelitic schist outside the mapped contact of the body. Pinch-and-swell structure of leucogranite sheets discordant to foliation suggest that waning plastic deformation was not finished at the time of emplacement of the Phillips pluton (Pressley and Brown, 1999). We infer from this that the exposure represents a cut through the pluton at a depth below the level of

the contemporary brittle–plastic transition, which is likely to be quite shallow in transpressive orogens that involve advection of mass and heat in magma (Ord and Hobbs, 1989).

At its margins, the Phillips pluton records no solid-state deformation of the kind commonly attributed to inflation by ballooning (Cloos, 1925; Holder, 1979; Marsh, 1982; Ramsay, 1989; Guglielmo, 1993). There is no discrete metamorphic aureole separable from the regional metamorphism. Although at amphibolite facies grade, the immediate country rocks are not ubiquitously migmatitic, although small areas of migmatite are mapped (Pressley and Brown, 1999). Migmatites of the WAD are exposed only a few km to the south-southwest (Fig. 2), however, where the elevation is lower. Based on the absence of a discrete contact metamorphic aureole and the concordancy between magmatic fabrics in the granite and the regional metamorphic fabrics in the surrounding rocks, we interpret emplacement of the Phillips pluton to have occurred during active deformation, synchronous with regional metamorphism. According to Brown and Solar (1998b), the pressure of metamorphism around the Phillips pluton was ~ 4 kbar [based on the production of sillimanite rather than andalusite by the reaction muscovite + staurolite + chlorite + quartz \rightarrow sillimanite + biotite + H₂O in pelitic schist (Guidotti, 1974; Guidotti et al., 1991), using the petrogenetic grid of Pattison and Tracy (1991); and, using the muscovite–almandine–biotite–sillimanite geobarometer (Holdaway and Mukhopadhyay, 1996), M.J. Holdaway, pers. commun., 1996].

Brown and Solar (1998b) interpret the Phillips pluton to be a steeply SE-dipping composite body with a hemi-ellipsoidal form in three dimensions, the long axis of which is inferred to plunge moderately northeast, similar to the mineral elongation lineation in the country rocks (Fig. 8, structure sections B–B' and C–C'). A funnel-shaped body has been sug-

Fig. 8. Map to show the relationship between granite plutons and the Central Maine belt shear zone system (modified after Brown and Solar, 1998b). Contours of residual gravity are taken from Carnese (1981). The 2 km contour of depth to the contact beneath the Lexington pluton is taken from Unger et al. (1989). AFZs are indicated by the grey ornament, and ACZs are unornamented; migmatite domains and plutons are indicated in various ornaments, given in Fig. 2. An indication of the extent of the metamorphic aureole surrounding each pluton is given by an appropriate isograd (see Brown and Solar, 1998b for details). B–B' and C–C' are lines of true-scale sections that cross the Phillips pluton; these are shown beneath the map. The N–S longitudinal section (D–D') and horizontal slices through the Lexington pluton are based on models in Unger et al. (1989).

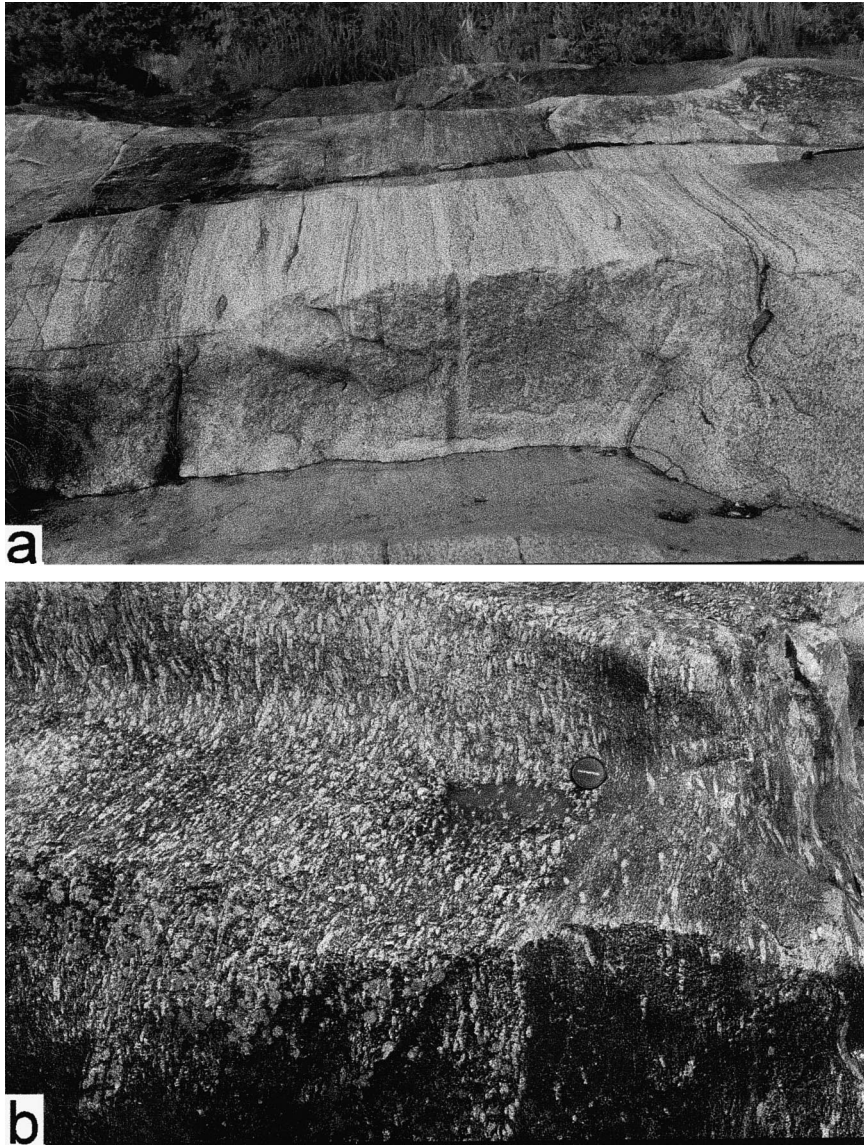


Fig. 9. (a) View to the northeast of magmatic layering and foliation within leucogranite of the Phillips pluton, north of the bridge on Maine Route 149, Phillips, west-central Maine, USA. (b) View to the southwest of magmatic foliation in porphyritic granodiorite of the Lexington pluton, Sandy Stream, Lexington, west-central Maine, USA.

gested in a three-dimensional geologic model constructed from combined geophysical and geological data (Unger et al., 1989). The -10 mGal residual gravity contour (Carnese, 1981) is taken to outline the root zone of the pluton (Fig. 8). We infer that melt ponded and crystallized within the ACZ to form the Phillips pluton. It is plausible that the Phillips pluton extended laterally at shallower levels as a tab-

ular pluton removed by erosion, but we have no information to constrain such speculation (cf. Guidotti and Holdaway, 1993).

4.2. *The Lexington pluton*

The Lexington pluton, which is the thickest pluton in the area, comprises a northern and central-south-

ern lobe (Figs. 2 and 8). The northern lobe, which is elongate N–S with axial dimensions of 15×12 km, is composed of biotite granite; it exhibits an apparent dextral offset with respect to the central-southern lobe. The central-southern lobe, which has axial dimensions of 20×10 km, is composed of porphyritic and two-mica granites. Williamson and Seaman (1996) interpret magma mingling textures at the deepest levels exposed (at lower elevations) to represent interaction between infusions of mafic magma and resident partially crystallized granite. A variably developed, NE-striking, steeply dipping magmatic fabric is present throughout the central lobe of the pluton (Fig. 9b); this is consistent in strike and dip with the regionally developed metamorphic fabrics outside the pluton. The northern lobe is in the ACZ to the northwest of the central AFZ; a thermal aureole was produced up to ≈ 1.5 km wide (Dickerson and Holdaway, 1989). Based on the succession of metamorphic mineral assemblages developed toward the contact in the thermal aureole in muscovite–quartz–ilmenite–graphite-bearing pelitic schist [cordierite + biotite + chlorite, andalusite + cordierite + biotite, and sillimanite + K-feldspar + cordierite + biotite; from Dickerson and Holdaway (1989)], Brown and Solar (1998b) estimated metamorphic P of ~ 3 kbar using the petrogenetic grid of Pattison and Tracy (1991).

The central-southern lobe cuts across the strike of the central AFZ (Figs. 2 and 8). Around the central-southern lobe, the thermal aureole expands from ~ 1.5 km at the central part to ~ 8 km on both the west-southwest and east-northeast of the southern part, before narrowing to ~ 1.5 km at the south end of the pluton (Dickerson and Holdaway, 1989). Based on the succession of metamorphic mineral assemblages toward the contact in muscovite–quartz–ilmenite–graphite-bearing pelitic schist [andalusite + staurolite + biotite \pm garnet, andalusite + biotite + garnet, and sillimanite + biotite + garnet; from Dickerson and Holdaway (1989)], Brown and Solar (1998b) estimated metamorphic P of 3–3.5 kbar using the petrogenetic grid of Pattison and Tracy (1991). The pluton is characterized by a moderate-to-large negative gravity anomaly (Unger et al., 1989), modeling of which yields moderately inward-dipping walls along the west-southwestern and east-northeastern sides of the central-southern lobe

of the pluton. Since there is no geophysical evidence in support of the pluton extending below the wide thermal aureole to the west and east of the southern part, Stewart (1989) postulated that originally the pluton was more extensive in a WSW–ENE direction above the thermal aureole. If correct, this implies a shallow, inward-dipping pluton floor to the west-southwestern and east-northeastern sides of the exposed central-southern lobe, which extended outward and upward to an unknown level in the crust above the exposed level. This raises the minimum width of this lobe to at least 35 km. Based on this interpretation, we have projected the possible shape of such a tabular head at a level 2 km above the present surface, and this is shown in Fig. 8.

Modeling by Unger et al. (1989) suggests that the northern lobe presently is ~ 12 km thick, with steep inward-dipping contacts, in comparison with the central-southern lobe, the present thickness of which thins from ~ 6 to ~ 3 km across the strike of the central AFZ (Fig. 8, section D–D'). Thus, the Lexington pluton has a complex three-dimensional form and a hybrid geometry, with a hemi-ellipsoidal northern lobe and an elongate tabular central-southern lobe. The level of emplacement as exposed is interpreted to have been close to the contemporary brittle–plastic transition. Brown and Solar (1998b) suggest that the northern lobe was formed by crystallization of melt that ponded in the ACZ. In contrast, however, if the central-southern lobe, which cross-cuts the central AFZ, was more laterally extensive within 2 km above the present erosion level, this part of the pluton may have been emplaced by magma-fracture and lateral flow to the south-southeast as a (sub-)horizontal sheet that propagated from a feeder zone (Brown and Solar, 1998b). Space creation to allow inflation could have occurred by sinking of the pluton floor and/or lifting the roof (e.g., Cruden, 1998). Seismic reflection data show that the floor of the pluton is not sharp against the wall rock; there is a zone of ~ 2 km thick where energy is weakly reflected, which is inconsistent with expectations for homogeneous granite (Stewart, 1989). One plausible interpretation of this zone is that it comprises sheets of granite interleaved with country rock.

4.3. Discussion

The Phillips pluton was constructed in an ACZ as ascent became inhibited (Pressley and Brown, 1999). The Lexington pluton is interpreted to represent a hybrid emplacement mechanism in which one part (the northern lobe) has maintained a deep root, while in the other part (the central-southern lobe) melt was emplaced by (sub-)horizontal flow across strike of the moderate-to-steeply dipping country rocks. Inflation of the central-southern lobe must have involved largely vertical displacements, but whether these displacements were accommodated solely by sinking of the pluton floor or whether a component of lifting the roof occurred is unknown.

For any pluton, a question is raised about the original size in comparison with the size that is now exposed, or how much of the pluton volume has been lost to erosion. We call this the ‘cut effect’. The cut effect raises an additional question concerning what is meant by the ‘depth of emplacement’, which commonly is taken to be the depth at the level of the cut. For example, for a pluton composed of a 5-km-thick horizontal tabular head and a 5-km-deep root zone, the maximum difference in depth of emplacement is recorded as ~ 3 kbar difference in P in the contact metamorphosed rocks from roof to floor. In any terrane, plutons have variable three-dimensional form with depth, which will necessarily vary from pluton to pluton and terrane to terrane as a function of tectonic history and crustal rheology during pluton emplacement. Nonetheless, for any pluton, cuts at different levels yield different map shapes and sizes. Finally, there is the issue of the relationship between plutons and regional-scale structures, which also may depend on the level of cut.

To illustrate these points, we show four cuts through the Lexington pluton in Fig. 8, one of which is the map pattern and three that are interpreted, one projection upward based on the width of the contact metamorphic aureole around the central-southern lobe and two cuts through the three-dimensional geophysical model of Stewart (1989) at -2 km and -4 km, respectively. These cuts show that the shape and area of the pluton change dramatically over a vertical interval of 6 km. Thus, at deeper exposed crustal levels in some terranes, plutons may be lower cuts through bodies with similar original

three-dimensional form and ‘depth of emplacement’ to ones that exhibit higher cuts at shallower exposed crustal levels. In this context, we interpret the exposed part of the Phillips pluton to be a lower cut at a deeper exposed crustal level, consistent with an interpretation that it is the remains of a magma feeder channel to a larger pluton, whereas we interpret the exposed part of the Lexington pluton to be a higher cut at a shallower exposed crustal level, consistent with the larger volume of granite in what remains of the pluton (Figs. 2 and 8). Pluton contacts commonly are discordant at higher levels in a body, for example at the margins of the tabular head (e.g., the central-southern lobe of the Lexington pluton), but are commonly concordant with regional-scale structures when viewed in deeper cuts, for example in the root zone of such a pluton (as exemplified, perhaps, by the Phillips pluton). If the Phillips pluton does represent the ascent conduit for a more extensive granite with a horizontal tabular head that was removed by erosion, then we presume that ascent became inhibited at the present level because the rate of pluton inflation had become negligible at a shallower level, perhaps due to solidification of the melt causing downward back-filling of the ascent conduit.

Finally, there is the contrast in contact metamorphic effect associated with each of the Lexington and Phillips plutons. Again, we relate the observed differences to the ‘cut effect’. Thus, metamorphic assemblages in the discrete aureole around the northern lobe of the Lexington pluton record pressures of ~ 3 kbar, whereas the aureole broadens in outcrop width across the central-southern lobe and the metamorphic mineral assemblages record pressures of 3–3.5 kbar. The broadening of the aureole width associated with the small increase in apparent pressure is consistent with Stewart’s (1989) postulate that the pluton was laterally more extensive above the present erosion level in its southern part. There is no discrete contact metamorphic aureole associated with the Phillips pluton, but mineral assemblages indicate the pressure of metamorphism to have been ~ 4 kbar. In map view, the Phillips pluton is similar in size and shape to the downward projection of the northern lobe of the Lexington pluton after removal of 2–4 km of overburden. If we assume that the Phillips pluton originally had a volume similar to that of the Lexington, then it is plausible that it

extended laterally above the present erosion level, as suggested by Guidotti and Holdaway (1993). Further, if the interpretation that the Phillips pluton at the present level of erosion represents a cut through a feeder channel to a larger pluton, then the passage of magma through this channel over an interval of time would create a regionally significant thermal effect in contrast with the discrete contact metamorphic aureoles associated with ponded magma in the upper crust.

5. Geochronology in west-central Maine

The Phillips and Lexington plutons are part of a suite of early Devonian plutons of granite s.l. in the northern Appalachian orogen. Recently, many of these plutons have been dated precisely, revealing an extensive suite of early Emsian plutons emplaced syntectonically into the thickening orogenic wedge (Bradley et al., 1998; Solar et al., 1998). This zone of plutonic activity stretches from eastern Maine southeast through the study area in western Maine (Bradley et al., 1998; Solar et al., 1998) and into New Hampshire and Massachusetts (Robinson and Tucker, 1996; Robinson et al., 1998).

The age of crystallization of granites in the Phillips pluton has been reported by Solar et al. (1998) and discussed by Pressley and Brown (1999); ages are quoted at 95% confidence. Two samples of leucogranite yielded U–Pb ages of 403.5 ± 1.6 Ma (zircon and monazite) and 402.7 ± 3.6 Ma (monazite). Two samples of granodiorite yielded U–Pb ages of 403.6 ± 2.2 Ma (zircon and monazite) and 404.8 ± 1.2 Ma (monazite). The weighted mean of data from all four samples yields an overall crystallization age of 403.8 ± 1.3 Ma at 95% confidence. Schlieric granite to the south of the Phillips pluton within the area of the WAD yielded a U–Pb age of 405.3 ± 1.8 Ma (zircon; Solar et al., 1998) that is the same as those of the granites within error. One sample of granite from the central-southern lobe of the Lexington pluton yielded a U–Pb age of 404.2 ± 1.8 Ma (zircon; Solar et al., 1998). The ca. 404 Ma age for the Lexington pluton is consistent with a Rb–Sr whole-rock age of 399 ± 6 Ma (Gaudette and Boone, 1985; see also Dickerson and Holdaway, 1989). Magmatic zircon and mon-

azite separated from samples of three synkinematic m-scale leucogranite sheets lodged within the central AFZ, from south to north along the strike of the zone, yielded ages of 408.2 ± 2.5 Ma, 407.9 ± 1.9 Ma and 404.3 ± 1.9 Ma, interpreted to date crystallization closely (Solar et al., 1998). The last of these samples was taken from a m-scale sheet that is part of the highly elongate multiply sheeted composite elliptical pluton referred to above. These granite crystallization ages are similar to U–Pb monazite ages from samples of staurolite zone pelitic schist of $405 - 399 \pm 2$ Ma (Smith and Barreiro, 1990), further supporting magma intrusion during regional metamorphism. Thus, recent precise age data support a model based on feedback relations between deformation, metamorphism, and granite ascent through the crust (Solar et al., 1998).

6. A general model

Based on the observations presented above, we propose a model for melt ascent and emplacement that may have more general applicability to other obliquely convergent (transpressive) orogens. To achieve this goal, observations from the study area in west-central Maine are generalized, but specific components of the model are directly related to the examples described, both for clarity and to ensure compliance with the natural examples. First we review important background concerning the thermal structure of transpressive orogens, the melting regime, melt flow in actively deforming orogenic crust and issues that relate to pluton construction.

6.1. Thermal structure of transpressive orogens

Metamorphism in transpressive orogens typically is syntectonic; it varies from medium-pressure (kyanite–sillimanite) to low-pressure (andalusite–sillimanite) type. Clockwise pressure–temperature paths are characteristic (e.g., Thompson et al., 1997; Jamieson et al., 1998; Huerta et al., 1999), and result from the combined effects of: (1) material transfer within the orogen that advects hot crust to shallow depths and heat conduction to the surface during syntectonic erosion of the thickening orogen; (2) increased radioactive heat generation due to crustal

thickening; (3) dissipation of mechanical energy generated during deformation; and (4) at temperatures higher than the solidus temperature, increased strain rates due to weakening in the presence of melt. The initial distribution of radioactive heat production with depth, including the location of any anomalous heat-producing layers, is an important variable (e.g., Chamberlain and Sonder, 1990), and recent modeling suggests that shear-heating during thrusting may be more important than realized previously (Harrison et al., 1997, 1998; Nabelek and Liu, 1999). These processes strongly perturb the geothermal gradient by displacing isotherms toward the surface to create a thermal antiform, which forms a near-isothermal corridor along the core of the orogen (e.g., Royden, 1993; Huerta et al., 1996, 1998, 1999; Thompson et al., 1997; Jamieson et al., 1998). Because of this coupled mechanical and thermal evolution of transpressive orogens, temperatures in the middle crust exceed those at which anatexis is initiated in many common crustal rock types (Fig. 10).

For the Acadian metamorphic belt of the northern Appalachians, which is characterized by elevated modern-day heat flow ($\sim 65 \text{ mW m}^{-2}$) and high heat production ($\sim 3.5 \times 10^{-6} \text{ W m}^{-3}$), metamorphic field gradients suggest high-to-moderate rates of temperature change, but reveal only small variations in pressure. The stratigraphic sequence includes formations with high heat production, a consequence of high U and Th contents fixed in strongly reduced sediments of the precursor anoxic basin (Chamberlain and Sonder, 1990). Oblique translation during contractional deformation thickened the stratigraphic sequence and displaced isotherms toward the surface, to create the thermal structure imaged by the 'migmatite front' (e.g., Fig. 3, solidus), essentially an isothermal surface given the high dP/dT slope of the beginning of melting in most crustal protoliths. Melt transport to progressively shallower crustal levels by differential stress-induced processes and buoyancy helps propagate the thermal corridor upward by advecting of heat into the upper crust.

Once melt is trapped and crystallized in a pluton, its source can be traced using isotopic fingerprinting, so that we can assess the volume of melt derived from different sources in the crust. We can use this information to determine whether the thermal perturbation associated with high-temperature metamor-

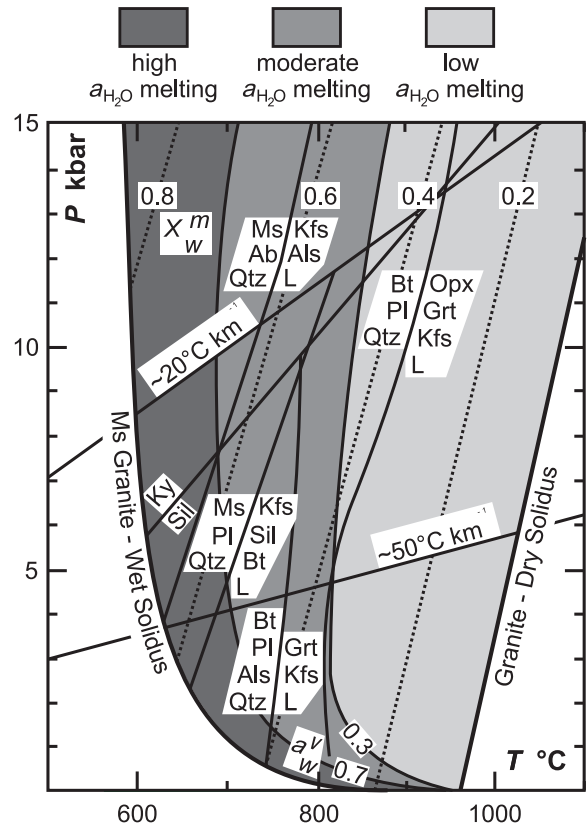


Fig. 10. P - T diagram of the anatectic zone, that region in P - T space above the wet solidus for crustal rocks of granitic composition in which melt may be present. The Ms granite-wet solidus is from Huang and Wyllie (1981), the reaction $Ms + Ab + Qtz \rightarrow Kfs + Als + L$ is from Petö (1976) and marks the lower T limit of plagioclase reactions (Thompson and Tracy, 1979), the reaction $Ms + Pl + Qtz \rightarrow Kfs + Sil + Bt + L$ is from Patiño Douce and Harris (1998), the reaction $Bt + Pl + Als + Qtz \rightarrow Grt + Kfs + L$ is from LeBreton and Thompson (1988) and the reaction $Bt + Pl + Qtz \rightarrow Opx + Grt + Kfs + L$ is from Vielzeuf and Montel (1994). The symbol X_w^m is used to denote the mole fraction of H_2O in the melt and is considered to equal the activity of H_2O in the melt (Burnham, 1979); isopleths of X_w^m are from Thompson (1996). The symbol a_w^v is used to denote activity of H_2O in the volatile phase, whereas a_{H_2O} refers to water activity in the environment; isopleths of a_w^v are from Thompson (1996).

phism extended to the Moho, reflected in voluminous granite magmatism from lower crustal or mixed (crust and mantle) sources, or was damped in the lower crust. In western Maine-eastern New Hampshire the absence of a significant volume of granite with a geochemical signature indicating deriva-

tion from basement inferred to underlie the Central Maine belt (e.g., Lathrop et al., 1996; Pressley and Brown, 1999; Brown and Pressley, 1999) is consistent with calculated intermediate-to-low reduced heat flow from the lower crust and mantle (Chamberlain and Sonder, 1990), and implies low thermal gradients in the lower crust under assumed granulite facies conditions. Thus, Acadian orogenesis involved redistribution of energy and mass within the crust, rather than addition of energy and mass by mantle processes.

6.2. *The melting regime*

The anatectic zone in continental crust during orogenesis is outlined in Fig. 10 by the 'Ms granite–wet solidus' and the 'granite–dry solidus'. Within this zone, melt may be present in appropriate lithologies, such as graywacke–shale (turbidite) protoliths. In these protoliths a significant volume of granite is generated by reduced $a_{\text{H}_2\text{O}}$ mica dehydration melting in the temperature interval $\sim 700\text{--}900^\circ\text{C}$ by melt-producing reactions such as those shown in Fig. 10. Once segregated from its residue the melt freezes at the wet solidus. Thus, there may exist a temperature interval of $\geq 100^\circ\text{C}$ below the temperature of the melt-producing reaction and above the temperature of the wet solidus that corresponds to a hot zone through which granite melt may migrate without solidifying (Fig. 10). It is this difference in temperatures between partial melting and freezing of the segregated liquid that enables granite melt to move through the anatectic zone. Thus, the anatectic zone is that portion of the crust with ambient temperature above the beginning of melting in wet granite, and in which melts of granite composition do not freeze; we do not imply that melt is pervasive throughout the anatectic zone.

During the evolution of transpressive orogens, crust in the anatectic zone that lies between geothermal gradients of $\sim 20^\circ\text{C km}^{-1}$ and $\sim 50^\circ\text{C km}^{-1}$ will be an important source region for granite magma, and a weak zone in which deformation may be preferentially localized. Deformation in the middle-lower crust is accommodated by plastic strain of these partially molten rocks that may involve melt loss from the anatectic zone (Brown, 1995). As a result, syntectonic transfer of heat to the upper crust

due to melt transport is significant in many contractional orogens (e.g., De Yoreo et al., 1989a,b, 1991).

6.3. *Melt flow in actively deforming crust*

During orogenesis, melting occurs in a dynamic environment. Magma migration depends on processes at two scales. At the microscale, melt is generated at grain boundaries and segregation likely is driven by surface tension, whereas at the macroscale we are concerned with porous and conduit flow in a deforming medium [called pervasive flow by Collins and Sawyer (1996), Weinberg (1999) and Vanderhaeghe (1999)]. It is likely that deformation controls sites of initial melting (e.g., Hand and Dirks, 1992; Brown and Solar, 1998a), and that the presence of melt aids progressive deformation (e.g., Hollister and Crawford, 1986; Davidson et al., 1992; Brown, 1995; Brown and Dallmeyer, 1996; Brown and Solar, 1998a). Thus, flow of melt in crustal materials at depths below the brittle–plastic transition, at temperatures above the solidus, is coupled with plastic strain of those materials. The flow is driven by pressure gradients generated by tectonic stresses (smaller distances) and buoyancy (larger distances) (e.g., Rutter, 1997; Bagdassarov and Dorfman, 1998). Experimental modeling has confirmed that differential stress-induced melt migration, coupled with shear-enhanced compaction of the residual matrix, more efficiently leads to accumulation of melt in layers and pods than segregation of melt by buoyancy-driven compaction (e.g., Cooper, 1990; Rushmer, 1995; Rutter and Neumann, 1995; Bagdassarov et al., 1996).

In anisotropic crust, differential stresses lead to heterogeneous deformation at all scales, which creates structural heterogeneities and pressure gradients to drive melt from zones of generation to sites of accumulation during syntectonic anatexis (e.g., Brown, 1994; Sawyer, 1994; Collins and Sawyer, 1996; Rutter, 1997; Bagdassarov and Dorfman, 1998). Deformation of partially molten crust will lead to periodically connected melt flow networks due to buildup of melt pressure (e.g., Brown and Rushmer, 1997; Weinberg and Searle, 1998; Brown and Solar, 1998b), which will enable melt escape. In effect, transpressive orogens become crustal-scale shear-

zone systems with a characteristic evolving thermal structure that creates a hot corridor to control and localize granite ascent paths.

6.4. *Pluton construction*

At the emplacement site, the style of pluton assembly and the preservation of geochemical heterogeneity or its erasure by homogenization among successive melt batches depends on rates of ascent and emplacement, and rates of inflation and solidification (e.g., Brown and Solar, 1998b; Pressley and Brown, 1999). At the extremes, composite structure may develop if an individual batch of melt crystallizes before the arrival of a subsequent batch of melt, potentially preserving heterogeneity, whereas successive arrivals of melt batches before extensive crystallization is conducive to mingling and mixing, potentially leading to homogenization. The main bodies of many plutons appear to have formed from magma that crystallized slowly, so that incoming batches of melt have had the chance to mix, although the pluton still may exhibit compositional zoning developed as it crystallized from the margins inward. For example, in the granite complexes of the Fichtelgebirge (Germany and Czech Republic) the general geochemical zonation pattern is the result of a combination of multiple injections of single magma batches and in situ differentiation during magma emplacement (Hecht et al., 1997). In contrast, one might expect small plutons or the early formed (marginal?) parts of large plutons to have composite or sheeted structure. Less common, however, are large tabular plutons with sheeted structure, although the Qôrqt granite complex of southern West Greenland (Brown et al., 1981) and the South Mountain Batholith in Nova Scotia (Benn et al., 1997, 1999) are notable examples of very large composite plutons constructed by multiple sub-horizontal m-scale sheets of granite. These sheeted plutons preserve the identity of individual melt batches. In the Manaslu Intrusive Complex of the Central Himalaya, however, the identity of individual batches is cryptic, the composite nature of the complex being identified through isotope geochemistry (Vidal et al., 1982) and Th–Pb ion microprobe dating of monazite (Harrison et al., 1999).

Root zones of plutons are interpreted to represent the feeder channels or plumbing beneath the

main body or tabular head of the pluton. They may exhibit composite structure if the feeder channels were backfilled piecemeal during the last stage of pluton construction, as one batch of magma at a time congeals before the next batch arrives, perhaps reflecting waning melt flow through the plumbing. Waning melt flow likely is a result of declining deformation and relaxation of the thermal structure, so magma gets stuck in the feeder channels. Root zones may exhibit homogeneous structure if melt flow into the plumbing is maintained but continued inflation of the pluton head cannot occur so that the feeder channel is filled with melt. The root zone may be compositionally zoned because of fractional crystallization processes driven by inward solidification. Alternatively, if crystallization of melt in the feeder channels is fast enough, in situ differentiation may be prevented, and unzoned granite will be the result. The root zone may exhibit a combination of these features, so that a series of cuts downward may exhibit a progression from homogeneous structure, unzoned or zoned, to composite structure if the last pulses of magma were spaced sufficiently apart to preserve individual identity by congealing.

6.5. *Summary of observations at different scales in western Maine–eastern New Hampshire*

At map scale we observe plutons of granite associated with discrete contact metamorphic aureoles in low-grade terranes, both in Maine (e.g., the Lexington pluton) and elsewhere (see the summary in Pattison and Tracy, 1991), and regional metamorphic terranes in which high-grade metamorphic zones are spatially related to plutons of granite, both in Maine (e.g., De Yoreo et al., 1989b) and elsewhere (see the summary in Pattison and Tracy, 1991). Any map represents a projection of the surface geology onto an arbitrary horizontal plane. Thus, within any map area plutons may vary in size and in their relations with regional-scale tectonic structures according to differences in crustal level exposed within the area of the map. For example, in western Maine, smaller plutons commonly are conformable with regional-scale structures, such as the Phillips pluton in an ACZ, whereas larger plutons commonly cut across regional structures, such as the Lexington pluton, which cuts across both AFZs and ACZs. The rela-

tive barometry between the aureole of the Lexington pluton and the regional metamorphism around the Phillips pluton is up to 1 kbar, and we have shown already that removing an additional ~ 4 km of crust from the Lexington pluton yields a map pattern similar to that of the Phillips pluton consistent with such a difference in metamorphic pressure (Fig. 8).

Our preferred interpretation of relationships in the study area is the following (Fig. 11). Small granites, such as the Phillips pluton, represent more deeply eroded bodies. They correspond to cuts through the root zones interpreted from gravity data to be beneath laterally extensive plutons (Fig. 11c), which are inferred to have been magma feeder channels by which new batches of magma became part of the pluton (e.g., Vigneresse, 1988, 1995a,b; Benn et al., 1999). These feeder channels must connect the main body or tabular head of plutons to the migmatitic sources of the melts. We infer from the absence of migmatite immediately around the exposed cut through the Phillips pluton, however, and the fact that it continues for several km at depth, as interpreted from the gravity anomaly, that we see something close to a ‘middle cut’ through the feeder

channel to a once larger pluton. Whatever volume of magma might have passed through this feeder channel, at the level we see it was insufficient to raise the adjacent wall rocks above the solidus for wet granite to generate migmatites. In contrast, larger plutons associated with discrete contact metamorphic aureoles represent cuts through bodies at shallower levels in the crust closer to the tops of plutons (Fig. 11a,b).

At the outcrop scale we observe decametric to metric bodies of granite associated with migmatites and in which the form of the body was controlled by the tectonic structures (Fig. 11d–f). Thus, in AFZs we find stromatic migmatite that recorded flattening strain, which is associated with generally concordant planar sheet-like bodies of granite (e.g., Fig. 4), and in ACZs we find inhomogeneous migmatite that recorded constrictional strain, which is associated with rod-shaped leucosomes and cylindrical bodies of granite (e.g., Figs. 6 and 7). Within individual outcrops in migmatite terranes, the form of the leucosomes reflects the shape of the apparent tectonic strain ellipsoid recorded by fabrics in the host rock (although the planar leucosomes and sheet-like granites of the AFZs do exploit the

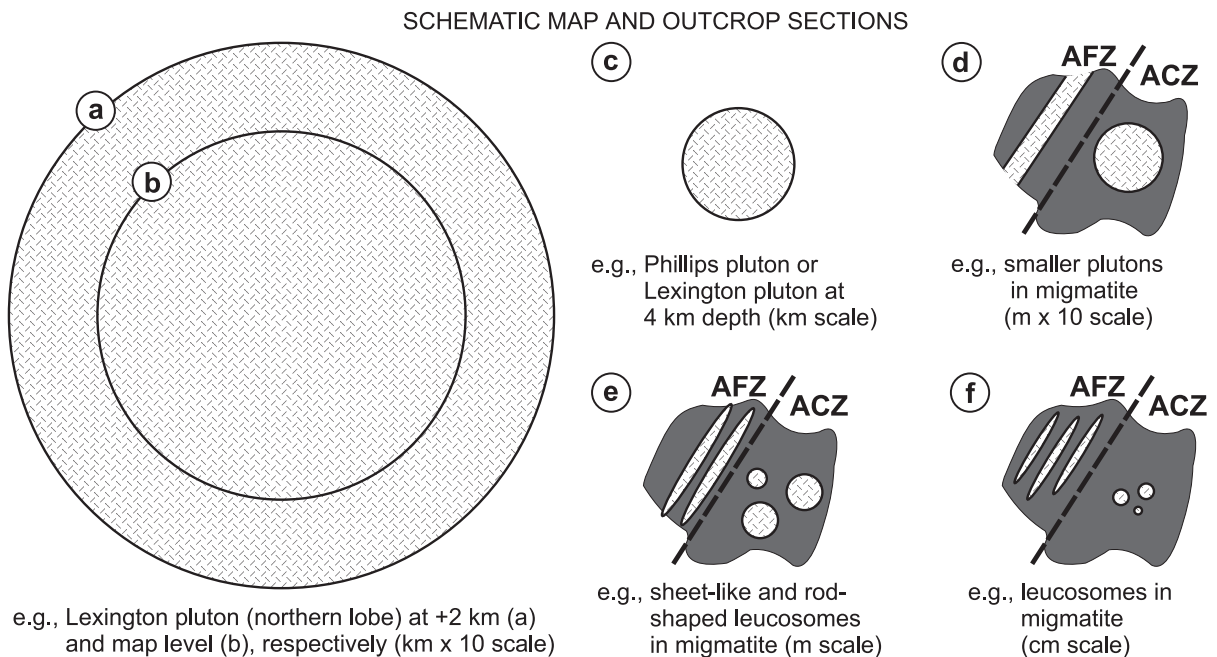


Fig. 11. Summary of observations using schematic map (horizontal) sections through plutons and outcrop (horizontal or oblique) sections through migmatites (see text for further discussion).

mechanical anisotropy, the pinch-and-swell structures and absence of solid-state fabrics suggest that deformation and emplacement were synchronous). We infer that the three-dimensional form of melt-escape paths in transpressive orogens is controlled by the contemporaneous deformation and is governed by strain partitioning. *Q.E.D.* magma ascent in obliquely convergent (transpressive) orogens is a syntectonic process, and thus pluton construction also must be a syntectonic process when viewed at the crustal scale, in spite of the local discordances between pluton contacts and regional-scale structures (cf. Karlstrom, 1989; Hutton, 1992; Brown, 1994; Vigneresse, 1995a,b; Benn et al., 1997, 1999; Brown and Solar, 1998b).

To the southwest of the Phillips pluton, the WAD is poorly exposed; although mapped by Moench and Pankiwskyj (1988) as part of the Phillips pluton, Brown and Solar (1998b) (see also Pressley and Brown, 1999) interpret it to be composed of stromatic migmatite and inhomogeneous migmatite with lenses of schlieric granite. Given the ubiquitous moderate-to-steeply NE-plunging mineral elongation lineation in the CMB rocks (Solar and Brown, 1999a), it is implicit that rocks similar to these stromatic migmatites and inhomogeneous migmatites with lenses of schlieric granite exposed immediately south of the Phillips pluton (Fig. 2) plunge underneath the pluton. Geochemical data reported from the Phillips pluton support field evidence of its composite nature, particularly the isotopic composition of Nd that suggests that the pluton is composed of multiple batches of melt (Pressley and Brown, 1999; Brown and Pressley, 1999). Furthermore, these authors showed that the leucogranite comprising most of the pluton was derived from a source with similar isotopic composition to the surrounding CMB rocks, although the minor granodiorite has an isotopic composition compatible with derivation from Avalon-like crust inferred to underlie the CMB rocks. These data are consistent with the inference that the deepest part of the Phillips pluton is close to or transitional into residual migmatites that sourced the common leucogranite of the exposed pluton. This interpretation implies that there are axial culminations along the hinge line of the thermal antiform represented by the 'migmatite front' that focused melt accumulation to feed plutons.

We postulate that migmatites occur immediately beneath the northern lobe of the Lexington pluton, at a depth of ~ 12 km, given the depth of the northern lobe as modeled by Unger et al. (1989). For any enhanced geotherm appropriate to this high-temperature, low-pressure metamorphic belt, it is reasonable to expect upper amphibolite facies metamorphic conditions at a depth appropriate to the inferred bottom of the northern lobe of the Lexington pluton. Both the northern lobe of the Lexington pluton and the Phillips pluton are found in zones of apparent constriction. We infer that melt accumulates preferentially in these zones and is driven out of the zones of apparent flattening by the enhanced deformation (Brown and Solar, 1998a,b).

6.6. Time-integrated schematic cross-section based on relations in western Maine — eastern New Hampshire

Modeling of convergent orogens provides insight about the evolution and decay of the thermal structure with time in the orogenic crust (Royden, 1993; Huerta et al., 1996, 1998, 1999; Thompson et al., 1997; Jamieson et al., 1998). At the peak of the thermal evolution, the solidus for granite melt (represented by the Ms granite wet solidus in Fig. 10) will be at the shallowest level in the crust within the core of the orogenic belt. At this time, melt transferring through the orogenic crust in planar and pipe-like conduits can reach shallow levels without freezing, and if the melt has accumulated into large enough batches it may pass into the unmelted crust (crust that did not achieve temperatures appropriate to the wet solidus of granite) before arrest at the site of a future pluton. The mechanism of this transfer might involve melt-enhanced embrittlement (Davidson et al., 1994), since the solidus represents the boundary to the anatectic zone with its interconnected melt-filled porosity. Viscous compaction within the anatectic zone is likely to generate strong variations in pressure near the solidus, which will enable deformation at the melt front to be essentially elastic in character (Connolly and Podladchikov, 1998). Under this condition melt may be transported into the unmelted (zero-porosity, subsolidus) crust by an elastic shock. We speculate that the physical expression of this phenomenon may be sheet-like bodies of granite

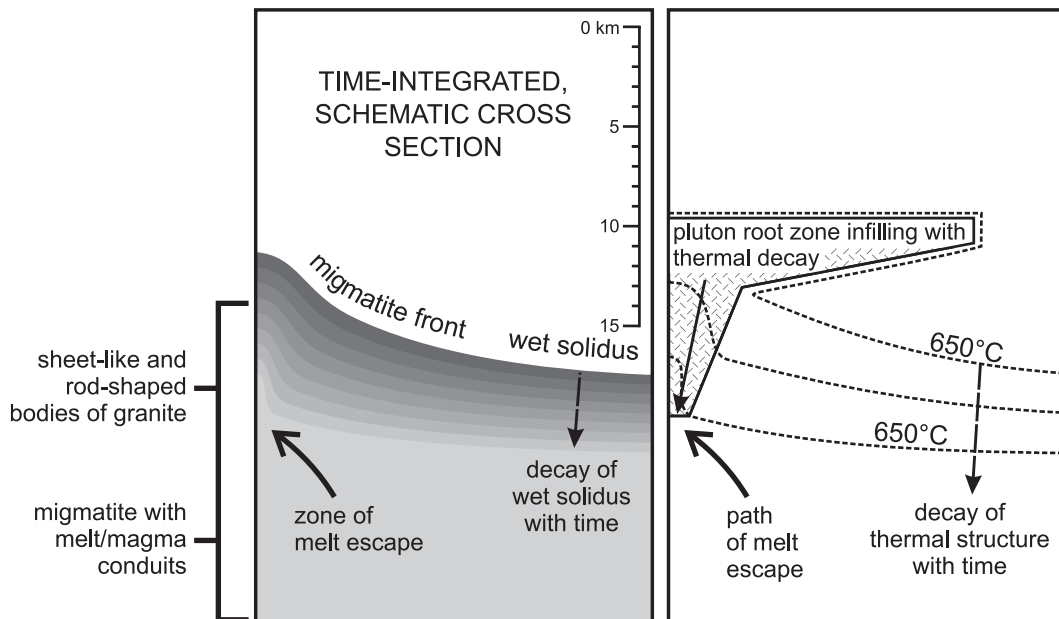


Fig. 12. Time-integrated, schematic cross-section through orogenic crust to illustrate the relations between the thermal evolution of the anatectic zone and the construction of a pluton composed of a tabular head and a root zone that extends down to migmatites of the anatectic zone (see text for further discussion). The cross-section is drawn vertical in a plane parallel to the mineral elongation lineation. The position of the 650°C isotherm in the pluton is generalized, based on the results of modeling presented by Furlong et al. (1991).

that occupy tensile and dilatant shear fractures in rocks of the AFZs.

In the ACZs, amplification of flow instabilities across the solidus, which represents an unstable interface, may be a more appropriate mechanism of melt ascent, as discussed by Paterson and Miller (1998). Whitehead and Helfrich (1991) have investigated the dynamics of flow instabilities that develop increasing resistance as they advance into cooler regions across an interface. In their experiments, the number of advancing fingers rapidly decreased with time to one, and the flow became focused. In the crustal environment, thermal softening will displace the solidus farther up in the crust, to localize the thermal zone in which ascent of melt will preferentially occur. The style of pluton construction then will be controlled by the rate of arrival of melt versus the rate of crystallization of the accumulated melt, as discussed above under Section 6.4, and the eventual decay of the thermal structure.

Given our inference above that the exposed level of the Lexington pluton likely was emplaced around the brittle–plastic transition, and the exposed level

of the Phillips pluton likely was emplaced below the brittle–plastic transition, for a geotherm consistent with these inferences the northern lobe of the Lexington pluton and the Phillips pluton may pass gradationally into residual inhomogeneous migmatite at depth beneath the present erosion surface. As orogenic deformation wanes, so the thermal structure decays, the height to which any batch of melt can ascend moves downward in the crust, and the periods between arrivals of melt batches into the magma feeder channel at the base of the pluton may become longer. In this circumstance, individual batches of magma may freeze before the arrival of subsequent batches, which will construct a downward-growing composite root zone that progressively occupies the magma feeder channel beneath a large pluton (Fig. 12). Thus, pluton construction is ended by downward congelation of granite melt in the magma feeder channel during the waning stages of orogeny. Although this is one alternative among a range of possible scenarios, we speculate it is a reasonable interpretation of the data in western Maine and may have application elsewhere in transpressive orogens.

6.7. Combining the different views of granite ascent and emplacement

In producing a model that relates generation of melt to ascent and emplacement, it is necessary to project relationships observed at the erosion surface to depth. Differences in structural level exposed across an area, the vertical relief and the quality of geophysical investigations to determine the sub-surface structure are limitations on what we can achieve. Within the study area, although exposure generally is poor, it is nonetheless adequate to establish geological relationships, vertical relief is ~1 km and the difference in structural levels corresponds to ~1 kbar. Furthermore, there are extensive regional-scale geophysical data sets supplemented by more local studies. Within these factors and data sets, our

model does not violate known information, but it does require further testing.

The schematic map and outcrop sections of Fig. 11 have been combined with the time-integrated schematic cross-section of Fig. 12 to provide a three-dimensional understanding of our general model of granite ascent and emplacement in Fig. 13. At shallower contemporary levels in the crust we expect to see the maximum areal extent of granite plutons. With each successively deeper slice the pluton becomes smaller, and the pluton may be more likely to be composite in structure, as opposed to homogeneous in structure, in passing from the main tabular body to the root zone. Ultimately the pluton passes downward into the source region represented by residual migmatites that preserve outcrop-scale melt-escape structures.

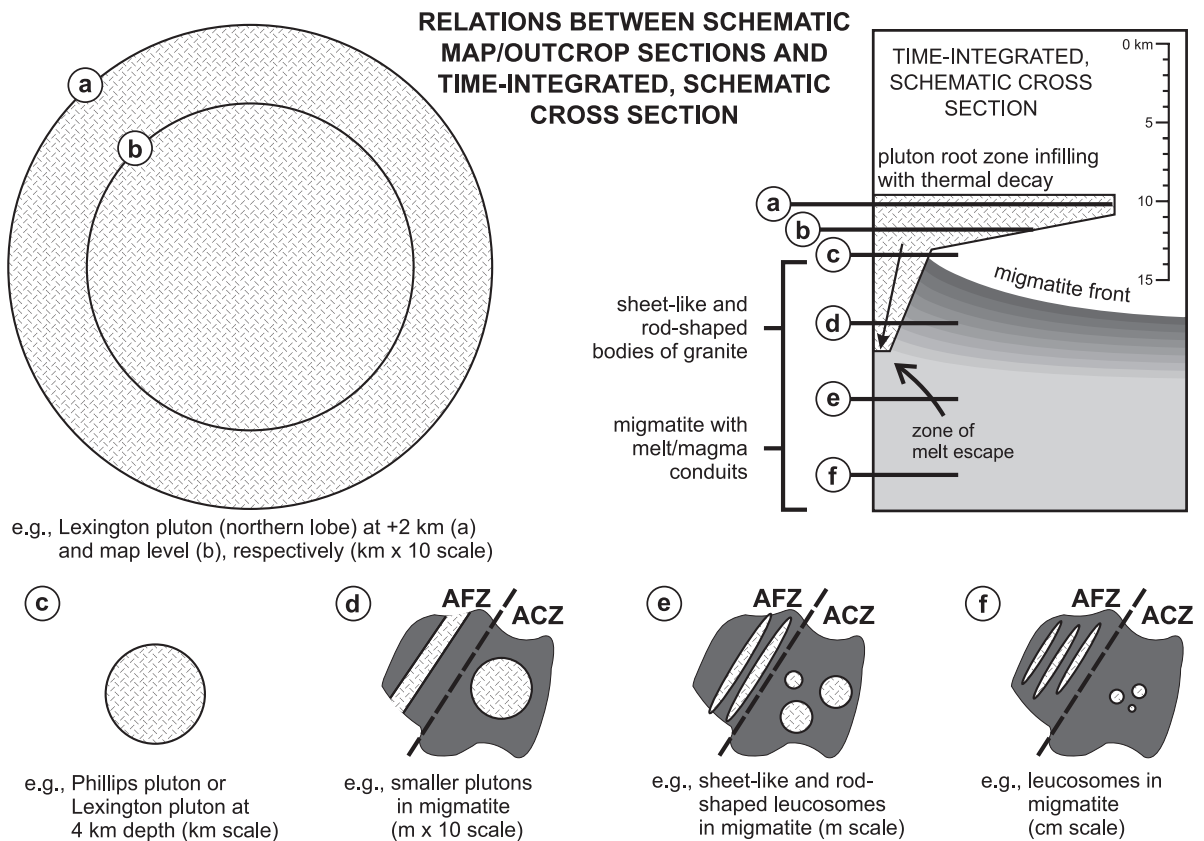


Fig. 13. Relations between schematic map and outcrop sections and the time-integrated, schematic cross-section through orogenic crust, based on the schema in Figs. 11 and 12, from which the general model of granite ascent and emplacement discussed in the text has been developed.

6.8. Focusing mechanisms

A principal difficulty in any model of granite ascent and emplacement is to focus the flow of melt in the source to feed melt through the ascent conduit at rates that are sufficient to avoid solidification ($<10^5$ yr; see discussion in Clemens et al., 1997, and Weinberg, 1999). This is a non-trivial problem, for even a modest size pluton of 10^3 km³ volume derived from a metasedimentary source by ~ 10 – 20 vol.% melting requires a source region of up to 10^4 km³. If melt moves through the anatectic zone in the pervasive manner postulated in this paper, freezing is not a problem, and the antiformal thermal structure will help to focus melt accumulation. Based on the small number of root zones identified beneath individual large plutons using gravimetry (e.g., Vigneresse, 1988, 1995a), the focusing mechanism must involve a substantial horizontal component of melt flow through the source region. Furthermore, given the slow velocity of percolative melt flow (e.g., Brown et al., 1995b), melt drained from the source by pulsed flow in batches in planar and/or pipe-like conduits must have been extracted previously from the pore structure and must have been available in a connected melt flow network composed of smaller-scale planar and/or pipe-like conduits (cf. Rubin, 1998; Weinberg, 1999). The intimate relation between migmatite leucosome and granite in melt-escape structures is significant (e.g., Figs. 4 and 7), and confirms the anticipated link between storage porosity (storage network) and the main ascent network (flow network). Our observations of field relationships and our interpretation of permeability networks and focused melt flow receive support from modeling (e.g., Miller, 1998).

As oblique translation during contractional deformation displaces isotherms to shallower depth in the crust, so melt can migrate to progressively higher crustal levels by differential stress-induced processes and buoyancy. Because the melt advects heat to these higher crustal levels as it migrates, the isotherms are pushed to even shallower depth (cf. Weinberg, 1999), which enables the zone of plastic deformation to expand to higher crustal levels in a feedback relation (cf. Brown and Solar, 1998a). Further, because the surface in three dimensions that corresponds to the outer limit of anatectic melt is essentially isothermal at pressures appropriate to the middle crust it reflects

the thermal structure of the deforming orogen. The geometry of this surface, which is not necessarily an isochronous feature, may be complex in detail, but its enveloping surface will approximate an antiformal structure, which may exhibit axial culminations and depressions. Culminations in the thermal antiformal are represented by the map outlines of migmatite domains, such as the TAD and WAD in western Maine (Figs. 2 and 3), and plutons that likely root into culminations at depth, assuming a shallow northeast plunge for the hinge line of the thermal antiformal. At temperatures above the solidus temperature, we expect that melt will migrate along the fabric parallel to the anisotropy of permeability (Brown and Solar, 1998a) until it reaches the solidus surface. Since the solidus is the limit of zero porosity for pervasive melt flow, at the solidus surface we expect melt to flow laterally toward axial culminations in the thermal antiformal. Since melt may drain preferentially from AFZs and accumulate in ACZs, we expect these axial culminations to occur in the ACZs. Our model is based on pervasive melt flow in the partially molten and deformable source (Stevenson and Scott, 1987; Sleep, 1988; Sawyer, 1994), by both porous flow and melt-assisted granular flow. In both cases we argue that granite frozen in channels was connected to the storage porosity represented by the migmatite leucosome to enable melt transport through the source. We avoid the issue of whether melt can be drained sufficiently rapidly from a partially molten source to sustain channel flow through subsolidus crust to infill a pluton (10^3 to 10^4 km⁻³) by allowing melt to accumulate in axial culminations of an antiformal solidus surface. This is necessary because channel flow must drain large concentrations (segregations) of melt if volumes large enough to form plutons are to escape the source (e.g., Rubin, 1998; Weinberg, 1999). Melt that escapes from these accumulation sites in axial culminations is likely able to cross a short segment of the subsolidus crust (Rubin, 1995) before freezing to begin the pluton construction process.

7. Conclusions

In western Maine, the Central Maine belt shear zone system is defined by NE-striking, steeply SE-dipping zones of apparent flattening strain (AFZs)

that anastomose around lenses of crust that have accommodated constrictional strain (ACZs), reflecting kinematic partitioning of flow during transpression (Solar and Brown, 1999b). Porphyroblast–matrix mineral microstructural relations demonstrate synchronous metamorphism and deformation (Solar and Brown, 1999a), to suggest feedback relations among mechanical and thermal processes in transpressive orogens. Within this context, our observations in the study area show that stromatic migmatite is found primarily within AFZs, and inhomogeneous migmatite is found within ACZs. Further, we have shown that the form of melt-escape structures is conformable with the shapes and orientations of the tectonic strain ellipsoids defined by the metamorphic mineral fabrics. Thus, sheet-like and cylindrical bodies of granite are associated with apparent flattening-to-plane strain and constrictional fabrics, respectively, to suggest that granite ascent was in planar and pipe-like conduits that reflect strain partitioning.

Magma ascent through migmatites is possible because oblique translation during contraction displaces isotherms upward in the orogenic crust to form a thermal antiform. Heat advected with the migrating melt promotes further amplification of the thermal antiform in a feedback relation that extends the zone of plastic deformation and melt migration to higher levels in the crust. Melt accumulation in axial culminations along the thermal antiform may enable melt-enhanced embrittlement and melt escape into the subsolidus crust, or melt may be expelled by elastic shock, or the solidus surface may develop instabilities that amplify into magma fingers or sheet-like protrusions during viscous flow. Thus, melt crosses a segment of subsolidus crust. Although the first batches to ascend beyond the solidus may suffer thermal death, later batches accumulate to construct a pluton.

Upper crustal plutons have (sub-)horizontal tabular geometries with floors that slope down to the ascent conduits. The tabular heads of these plutons cut across boundaries between structural zones, such as the Lexington pluton in western Maine. Ascent conduits are represented by ‘smaller’ plutons with composite structure and hemi-ellipsoidal form, these correspond to root zones identified using models of gravity anomalies. In western Maine, an example is the Phillips pluton, which is found within

an ACZ. At the crustal scale, granite ascent and emplacement in obliquely convergent (transpressive) orogens are inherently syntectonic processes, controlled by the contemporaneous deformation and the progressive development of strain fabrics. Syntectonic magma ascent helps heat transfer through the crust to provide thermal peaks characteristic of low-pressure metamorphism. Thus, even those plutons that apparently cross-cut the fabrics in map view are interpreted to be syntectonic.

Acknowledgements

We thank the conveners of the Special Session at the Spring AGU Meeting in May 1998 on ‘Granite Emplacement and Tectonics’, Keith Benn and Carol Simpson, for the opportunity to present this work as part of the session, and for the invitation to contribute to this Special Issue. We acknowledge helpful discussion on the regional geology of west-central Maine with many people, including many stimulating discussions in the field. Keith Benn and Roberto Weinberg provided supportive and very stimulating critical comments as reviewers, for which we are grateful. Nonetheless, the ideas presented in this paper are our own, and any infelicities that remain are our responsibility. We acknowledge partial support of this work from the Department of Geology, University of Maryland, the Geological Society of America Research Grants Program and NSF Grant EAR-9705858. We thank Jeanne Martin for skilled word processing support, and MB thanks her for her tolerance.

References

- Bagdassarov, N., Dorfman, A., 1998. Granite rheology: magma flow and melt migration. *J. Geol. Soc.*, London 155, 863–872.
- Bagdassarov, N.S., Dorfman, A.M., Dingwell, D.B., 1996. Modeling of melt segregation processes by high-temperature centric fusing of partially molten granites. I. Melt extraction by compaction and deformation. *Geophys. J. Int.* 127, 616–626.
- Bateman, R., 1984. On the role of diapirism in the segregation, ascent and final emplacement of granitoid magmas. *Tectonophysics* 110, 211–231.
- Benn, K., Horne, R.J., Kontak, D.J., Pignotta, G.S., Evans, N.G., 1997. Syn-Adian emplacement model for the South Mountain batholith, Meguma Terrane, Nova Scotia: magnetic fabric

- and structural analyses. *Geol. Soc. Am. Bull.* 109, 1279–1293.
- Benn, K., Odonne, F., de Saint Blanquat, M., 1998. Pluton emplacement during transpression in brittle crust: new views from analogue experiments. *Geology* 26, 1079–1082.
- Benn, K., Roest, W.R., Rochette, P., Evans, N.G., Pignotta, G.S., 1999. Geophysical and structural signatures of syntectonic batholith construction: the South Mountain Batholith, Meguma Terrane, Nova Scotia. *Geophys. J. Int.* 136, 144–158.
- Berger, A., Rosenberg, C., Schmid, S.M., 1996. Ascent, emplacement and exhumation of the Bergell pluton within the Southern Steep Belt of the Central Alps, Schweiz. *Mineral. Petrogr. Mitt.* 76, 357–382.
- Bittner, D., Schmeling, H., 1995. Numerical modeling of melting processes and induced diapirism in the lower crust. *Geophys. J. Int.* 123, 59–70.
- Bradley, D.C., Tucker, R.D., Lux, D.R., Harris, A.G., McGregor, D.C., 1998. Migration of the Acadian orogen and Foreland Basin across the Northern Appalachians. U.S. Geol. Surv. Open-File Report 98-770, 79 pp.
- Brown, M., 1994. The generation, segregation, ascent and emplacement of granite magma: the migmatite-to-crustally-derived granite connection in thickened orogens. *Earth-Sci. Rev.* 36, 83–130.
- Brown, M., 1995. The late-Precambrian geodynamic evolution of the Armorican segment of the Cadomian belt (France): distortion of an active continental margin during south-west directed convergence and subduction of a bathymetric high. *Geol. Fr.* 3, 3–22.
- Brown, M.A., Brown, M., 1997. What is the connectivity of melt in the anatexis zone? Problems and approaches. *Geol. Soc. Am., Abstr. Progr.* 29, A-91.
- Brown, M., Dallmeyer, R.D., 1996. Rapid Variscan exhumation and role of magma in core complex formation: southern Brittany metamorphic belt, France. *J. Metamorph. Geol.* 14, 361–379.
- Brown, M., Pressley, R.A., 1999. Crustal melting in nature: prosecuting source processes. *Phys. Chem. Earth A* 24, 305–316.
- Brown, M., Rushmer, T., 1997. The role of deformation in the movement of granitic melt: views from the laboratory and the field. In: Holness, M. (Ed.), *Deformation-enhanced Melt Segregation and Metamorphic Fluid Transport*. The Mineralogical Society Series 8, Chapman and Hall, London, pp. 111–144.
- Brown, M., Solar, G.S., 1998a. Shear zone systems and melts: feedback relations and self-organization in orogenic belts. *J. Struct. Geol.* 20, 211–227.
- Brown, M., Solar, G.S., 1998b. Granite ascent and emplacement during contractional deformation in convergent orogens. *J. Struct. Geol.* 20, 1365–1393.
- Brown, M., Friend, C.R.L., McGregor, V.R., Perkins, W.T., 1981. The late-Archaeoan Qôrqut granite complex of southern West Greenland. *J. Geophys. Res.* 86, 10617–10632.
- Brown, M., Rushmer, T., Sawyer, E., 1995a. Introduction to Special Section: Mechanisms and Consequences of Melt Segregation from Crustal Protoliths. *J. Geophys. Res.* 100, 15551–15563.
- Brown, M., Averkin, Y., McLellan, E., Sawyer, E., 1995b. Melt segregation in migmatites. *J. Geophys. Res.* 100, 15655–15679.
- Burnham, C.W., 1979. Magmas and hydrothermal fluids. In: Barnes, H.L. (Ed.), *Geochemistry of Hydrothermal Ore Deposits* (2nd ed.). Wiley-Interscience, New York, pp. 71–136.
- Carnese, M.J., 1981. Gravity Study of Intrusive Rocks in West-central Maine. M.S. Thesis, University of New Hampshire, Durham.
- Chamberlain, C.P., Sonder, L.J., 1990. Heat-producing elements and the thermal and baric patterns of metamorphic belts. *Science* 250, 763–769.
- Clemens, J.D., 1998. Observations on the origins and ascent mechanisms of granitic magmas. *J. Geol. Soc., London* 155, 843–851.
- Clemens, J.D., Mawer, C.K., 1992. Granitic magma transport by fracture propagation. *Tectonophysics* 204, 339–360.
- Clemens, J.D., Petford, N., Mawer, C.K., 1997. Ascent mechanisms of granitic magmas: causes and consequences. In: Holness, M.B. (Ed.), *Deformation-Enhanced Fluid Transport in the Earth's Crust and Mantle*. The Mineralogical Society Series 8, Chapman and Hall, London, pp. 145–172.
- Cloos, H., 1925. Einführung in die tektonische Behandlung magmatischer Erscheinungen (Granittektonik), I. Spezieller Teil. Das Riesengebirge in Schlesien. Bau, Bildung, und Oberflächengestaltung. Borntraeger, Berlin, 194 pp.
- Cocks, L.R.M., McKerrow, W.S., van Staal, C.R., 1997. The margins of Avalonia. *Geol. Mag.* 134, 627–636.
- Collins, W.J., Sawyer, E.W., 1996. Pervasive magma transfer through the lower-middle crust during non-coaxial compressional deformation: an alternative to diking. *J. Metamorph. Geol.* 14, 565–579.
- Collins, W.J., van Kranendonk, M.J., Teyssier, C., 1998. Partial convective overturn of Archaean crust in the east Pilbara Craton, Western Australia: driving mechanisms and tectonic implications. *J. Struct. Geol.* 20, 1405–1424.
- Connolly, J.A.D., Podladchikov, Yu.Yu., 1998. Compaction-driven fluid flow in viscoelastic rock. *Geodyn. Acta* 11, 55–84.
- Cooper, R.F., 1990. Differential stress-induced melt migration: an experimental approach. *J. Geophys. Res.* 95, 6979–6992.
- Cruden, A.R., 1988. Deformation around a rising diapir modeled by creeping flow past a sphere. *Tectonics* 7, 1091–1101.
- Cruden, A.R., 1998. On the emplacement of tabular plutons. *J. Geol. Soc., London* 155, 853–862.
- Davidson, C., Hollister, L.S., Schmid, S.M., 1992. Role of melt in the formation of a deep-crustal compressive shear zone: the MacLaren Glassier metamorphic belt, south-central Alaska. *Tectonics* 11, 348–359.
- Davidson, C., Schmid, S.M., Hollister, L.S., 1994. Role of melt during deformation in the deep crust. *Terra Nova* 6, 133–142.
- de Roo, J.A., van Staal, C.R., 1994. Transpression and recumbent folding: steep belts and flat belts in the Appalachian Central Mobile Belt of northern New Brunswick, Canada. *Geol. Soc. Bull.* 106, 541–552.
- De Yoreo, J.J., Lux, D.R., Guidotti, C.V., 1989a. The role of crustal anatexis and magma migration in regions of thickened continental crust. In: Daly, J.G., Cliff, R.A., Yardley, B.W.D.

- (Eds.), *Evolution of Metamorphic Belts*. Geol. Soc. London Spec. Publ. 43, 187–202.
- De Yoreo, J.J., Lux, D.R., Guidotti, C.V., Decker, E.R., Osberg, P.H., 1989b. The Acadian thermal history of western Maine. *J. Metamorph. Geol.* 7, 169–190.
- De Yoreo, J.J., Lux, D.R., Guidotti, C.V., 1991. Thermal modelling in low-pressure/high-temperature metamorphic belts. *Tectonophysics* 188, 209–238.
- Dickerson, R.P., Holdaway, M.J., 1989. Acadian metamorphism associated with the Lexington batholith, Bingham, Maine. *Am. J. Sci.* 289, 945–974.
- D'Lemos, R.S., Brown, M., Strachan, R.A., 1992. Granite magma generation, ascent and emplacement within a transpressional orogen. *J. Geol. Soc., London* 149, 487–490.
- Emerman, S.H., Marrett, R., 1990. Why dikes? *Geology* 18, 231–233.
- Eusden Jr., J.D., Barreiro, B., 1988. The timing of peak high-grade metamorphism in central-eastern New England. *Marit. Sediment. Atlantic Geol.* 24, 241–255.
- Furlong, K.P., Hanson, R.B., Bowers, J.R., 1991. Modeling thermal regimes. In: Kerrick, D.M. (Ed.), *Contact Metamorphism and its Reviews in Mineralogy* Vol. 26, Mineralogical Society of America, Washington, DC, pp. 437–505.
- Gaudette, H.E., Boone, G.M., 1985. Isotope age of the Lexington Batholith, constraints on timing of intrusion and Acadian metamorphism in western Maine. *Geol. Soc. Am., Abstr. Progr.* 17, 19–20.
- Glazner, A.F., 1991. Plutonism, oblique subduction and continental growth: an example from the Mesozoic of California. *Geology* 19, 784–786.
- Grocott, J., Brown, M., Dallmeyer, R.D., Taylor, G.K., Treloar, P.J., 1994. Mechanisms of continental growth in extensional arcs: an example from the Andean Plate Boundary Zone. *Geology* 22, 391–394.
- Grocott, J., Garde, A.A., Chadwick, B., Cruden, A.R., Swager, C., 1999. Emplacement of rapakivi granite and syenite by floor depression and roof uplift in the Palaeoproterozoic Ketilidian orogen, South Greenland. *J. Geol. Soc., London* 156, 15–24.
- Guglielmo, G., 1993. Interference between pluton expansion and non-coaxial tectonic deformation: three-dimensional computer model and field implications. *J. Struct. Geol.* 15, 593–608.
- Guidotti, C.V., 1974. Transition from staurolite to sillimanite zone, Rangeley Quadrangle, Maine. *Geol. Soc. Am. Bull.* 85, 475–490.
- Guidotti, C.V., 1989. Metamorphism in Maine: an overview. In: Tucker, R.D., Marvinney, R.G. (Eds.), *Studies in Maine Geology*, Vol. 3. Igneous and Metamorphic Geology. Maine Geological Survey, Maine Department of Conservation, pp. 1–19.
- Guidotti, C.V., Holdaway, M.J., 1993. Petrology and field relations of successive metamorphic events in pelites of west-central Maine. In: Cheney, J.T., Hepburn, J.D. (Eds.), *Fieldtrip Guidebook for the Northeastern United States*. Geological Society of America, Washington, DC, pp. L1–L26.
- Guidotti, C.V., Teichmann, F., Henry, D.J., 1991. Chlorite-bearing polymetamorphic metapelites in the Rangeley area, Maine. *Am. Mineral.* 76, 867–879.
- Guineberteau, B., Bouchez, J.L., Vigneresse, J.L., 1987. The Mortagne granite pluton (France) emplaced by pull-apart along a shear zone. Structural and gravimetric arguments and regional implication. *Geol. Soc. Am. Bull.* 99, 763–770.
- Hand, M., Dirks, P.H.G.M., 1992. The influence of deformation on the formation of axial-planar leucosomes and the segregation of small melt bodies within the migmatitic Napperby Gneiss, Central Australia. *J. Struct. Geol.* 14, 591–604.
- Harrison, T.M., Lovera, O.M., Grove, M., 1997. New insights into the origin of two contrasting Himalayan belts. *Geology* 25, 899–902.
- Harrison, T.M., Grove, M., Lovera, O.M., Catlos, E.J., 1998. A model for the origin of Himalayan anatexis and inverted metamorphism. *J. Geophys. Res.* 103, 27017–27032.
- Harrison, T.M., Grove, M., McKeegan, K.D., Coath, C.D., Lovera, O.M., Le Fort, P., 1999. Origin and episodic emplacement of the Manaslu Intrusive Complex, Central Himalaya. *J. Petrol.* 40, 3–19.
- Hecht, L., Vigneresse, J.L., Morteani, G., 1997. Constraints on the origin of zonation of the granite complexes in the Fichtelgebirge (Germany and Czech Republic): evidence from a gravity and geochemical study. *Geol. Rundsch.* 86 (Suppl.), S93–S109.
- Hogan, J.P., Gilbert, M.C., 1995. The A-type Mount Scott Granite sheet: importance of crustal magma traps. *J. Geophys. Res.* 100, 15779–15792.
- Holdaway, M.J., Mukhopadhyay, B., 1996. Redetermination of garnet and biotite margules parameters and recalibration of the garnet–biotite geothermometer and the muscovite–almandine–biotite–sillimanite (MABS) geobarometer. *Geol. Soc. Am. Annu. Mtg., Abstr. Progr.* 28, A-356.
- Holder, M.T., 1979. An emplacement mechanism for post-tectonic granites and implications for their geochemical features. In: Atherton, M.P., Tarney, J. (Eds.), *Origin of Granite Batholiths: Geochemical Evidence*. Shiva, Kent, UK, pp. 116–128.
- Holdsworth, R.E., McErlean, M.A., Strachan, R.A., 1999. The influence of country rock structural architecture during pluton emplacement: the Loch Loyal syenites, Scotland. *J. Geol. Soc., London* 156, 163–175.
- Hollister, L.H., Crawford, M.L., 1986. Melt-enhanced deformation: a major tectonic process. *Geology* 14, 558–561.
- Huang, W.L., Wyllie, P.J., 1981. Phase relationship of S-type granite with H₂O to 35 kbar: muscovite granite from Harney Peak, South Dakota. *J. Geophys. Res.* 86, 1015–1029.
- Huerta, A.D., Royden, L.H., Hodges, K.V., 1996. The interdependence of deformational and thermal processes in mountain belts. *Science* 273, 637–639.
- Huerta, A.D., Royden, L.H., Hodges, K.V., 1998. The thermal structure of collisional orogens as a response to accretion, erosion, and radiogenic heat. *J. Geophys. Res.* 103, 15287–15302.
- Huerta, A.D., Royden, L.H., Hodges, K.V., 1999. The effect of accretion, erosion, and radiogenic heat on the metamorphic evolution of collisional orogens. *J. Metamorph. Geol.* 17 (in press).
- Hutton, D.H.W., 1988. Granite emplacement mechanisms and

- tectonic controls: inferences from deformation studies. *Trans. R. Soc. Edinburgh: Earth Sci.* 79, 245–255.
- Hutton, D.H.W., 1990. A new mechanism of granite emplacement: intrusion in active extensional shear zones. *Nature* 343, 452–455.
- Hutton, D.H.W., 1992. Granite sheeted complexes: evidence for the dyking ascent mechanism. *Trans. R. Soc. Edinburgh: Earth Sci.* 83, 377–382.
- Hutton, D.H.W., 1996. The ‘space’ problem in the emplacement of granite. *Episodes* 19, 114–119.
- Ingram, G.M., Hutton, D.H.W., 1994. The Great Tonalite Sill: emplacement into a contractional shear zone and implications for Late Cretaceous to Early Eocene tectonics in southeastern Alaska and British Columbia. *Geol. Soc. Am. Bull.* 106, 715–728.
- Jamieson, R.A., Beaumont, C., Fullsack, P., Lee, B., 1998. Barrovian regional metamorphism: Where’s the heat? In: Treloar, P.J., O’Brien, P.J. (Eds.), *What Drives Metamorphism and Metamorphic Reactions?* *Geol. Soc. London Spec. Publ.* 138, 23–51.
- Karlstrom, K.E., 1989. Toward a syn-tectonic paradigm for granitoids. *Eos* 70, 762–763.
- Klepeis, K.A., Crawford, M.L., 1999. High-temperature arc-parallel normal faulting and transtension at the roots of an obliquely convergent orogen. *Geology* 27, 7–10.
- Lathrop, A.S., Blum, J.D., Chamberlain, C.P., 1996. Nd, Sr and O isotopic study of the petrogenesis of two syntectonic members of the New Hampshire Plutonic Series. *Contrib. Mineral. Petrol.* 124, 126–138.
- LeBreton, N., Thompson, A.B., 1988. Fluid-absent (dehydration) melting of biotite in metapelites in the early stage of crustal anatexis. *Contrib. Mineral. Petrol.* 99, 226–237.
- Lister, J.R., Kerr, R.C., 1991. Fluid-mechanical models of crack propagation and their application to magma transport in dykes. *J. Geophys. Res.* 96, 10049–10077.
- Lucas, S.B., St. Onge, M., 1995. Syn-tectonic magmatism and the development of compositional layering, Ungava Orogen (northern Quebec, Canada). *J. Struct. Geol.* 17, 475–491.
- Mahon, K.I., Harrison, T.M., Drew, D.A., 1988. Ascent of a granitoid diapir in a temperature varying medium. *J. Geophys. Res.* 93, 1174–1188.
- Marsh, B.D., 1982. On the mechanics of igneous diapirism, stoping, and zone melting. *Am. J. Sci.* 282, 808–855.
- Miller, H.G., Tuach, J., 1989. Gravity and magnetic signatures of the Ackley Granite Suite, southeastern Newfoundland: implications for magma emplacement. *Can. J. Earth Sci.* 26, 2697–2709.
- Miller, S.A., 1998. Evolution of permeability networks and focussed flow in hydrofracture-controlled systems: application to dehydration and melting. *Eos* 79 (Supp.), F281.
- Moench, R.H., Pankiwskyj, K.A., 1988. Geologic map of western interior Maine. *U.S. Geol. Surv., Misc. Invest. Map I-1692*.
- Moench, R.H., Boone, G.M., Bothner, W.A., Boudette, E.L., Hatch, N.L. Jr., Hussey, A.M. II, Marvinney, R.G., Aleinikoff, J.N., 1995. Geologic map of the Sherbrooke–Lewiston area, Maine, New Hampshire, and Vermont, United States, and Quebec Canada. *U.S. Geol. Surv. Misc. Invest. Ser. Map I-1898-D*, 56 pp.
- Morgan, S.S., Law, R.D., Nyman, M.W., 1998. Laccolith-like emplacement model for the Pappose Flat pluton based on porphyroblast–matrix analysis. *Geol. Soc. Am. Bull.* 110, 96–110.
- Musacchio, G., Mooney, W.D., Luetgert, J.H., 1997. Composition of the crust in the Grenville and Appalachian Provinces of North America inferred from V_P/V_S ratios. *J. Geophys. Res.* 102, 15225–15241.
- Nabelek, P.I., Liu, M., 1999. Petrogenesis of leucogranites in the Black Hills, South Dakota, as the consequence of shear-heating during thrusting. *Geology* 27, 523–526.
- Ord, A., Hobbs, D.E., 1989. Strength of the continental crust, detachment zones and the development of plastic instabilities. *Tectonophysics* 158, 269–289.
- Oxburgh, E.R., McRae, T., 1984. Physical constraints on magma contamination in the continental crust: an example, the Adamello Complex. *Philos. Trans. R. Soc. London A310*, 457–472.
- Paterson, S.R., Fowler Jr., T.K., 1993. Reexamining pluton emplacement processes. *J. Struct. Geol.* 15, 191–206.
- Paterson, S.R., Miller, R.B., 1998. Mid-crustal magmatic sheets in the Cascades Mountains, Washington: implications for magma ascent. *J. Struct. Geol.* 20, 1345–1363.
- Paterson, S.R., Fowler Jr., T.K., Miller, R.B., 1996. Pluton emplacement in arcs: a crustal-scale exchange process. *Trans. R. Soc. Edinburgh: Earth Sci.* 87, 115–123.
- Patiño Douce, A.E., Harris, N., 1998. Experimental constraints on Himalayan anatexis. *J. Petrol.* 39, 689–710.
- Pattison, D.R.M., Tracy, R.J., 1991. Phase equilibria and thermobarometry of metapelites. In: Kerrick, D.M. (Ed.), *Contact Metamorphism. Reviews in Mineralogy* 26, Mineralogical Society of America, Washington, DC, pp. 105–206.
- Petford, N., 1996. Dykes or diapirs? *Trans. R. Soc. Edinburgh: Earth Sci.* 87, 105–114.
- Petford, N., Koenders, M.A., 1998. Granular flow and viscous fluctuations in low Bagnold number granitic magmas. *J. Geol. Soc., London* 155, 873–881.
- Petö, P., 1976. An experimental investigation of melting relations involving muscovite and paragonite in the silica-saturated portion of the system $K_2O-Na_2O-SiO_2-H_2O$ to 15 kbar total pressure. *Progress in Experimental Petrology*, 3, NERC, London, pp. 41–45.
- Pressley, R.A., Brown, M., 1999. The Phillips Pluton, Maine, USA: evidence of heterogeneous crustal sources, and implications for granite ascent and emplacement mechanisms in convergent orogens. *Lithos* 41, 335–366.
- Ramsay, J.G., 1989. Emplacement kinematics of a granite diapir: the Chindamora batholith, Zimbabwe. *J. Struct. Geol.* 11, 191–209.
- Ratcliffe, N.M., Hames, W.E., Stanley, R.S., 1998. Interpretation of ages of arc magmatism, metamorphism, and collisional tectonics in the Taconian orogen of western New England. *Am. J. Sci.* 298, 791–797.
- Robinson, P., Tucker, R.D., 1996. The ‘Acadian’ in central New England: new problems based on U–Pb ages of igneous zircon

- and metamorphic monazite and sphene. *Geol. Soc. Am. Progr. Abstr.* 28 (3), 94.
- Robinson, P., Tucker, R.D., Bradley, D., Berry IV, H.N., Osberg, P.H., 1998. Paleozoic orogens in New England, USA. *Geol. Fören. Stockholm Förh.* 120, 119–148.
- Roman-Berdiel, T., Gapais, D., Brun, J.P., 1995. Analog models of laccolith formation. *J. Struct. Geol.* 17, 1337–1346.
- Rosenberg, C.L., Berger, A., Schmid, S.M., 1995. Observations from the floor of a granitoid pluton: inferences on the driving force of final emplacement. *Geology* 23, 443–446.
- Royden, L.H., 1993. The steady-state thermal structure of eroding orogenic belts and accretionary prisms. *J. Geophys. Res.* 98, 4487–4507.
- Rubin, A.M., 1993. Dikes vs. diapirs in viscoelastic rock. *Earth Planet. Sci. Lett.* 117, 653–670.
- Rubin, A.M., 1995. Getting granite dikes out of the source region. *J. Geophys. Res.* 100, 5911–5929.
- Rubin, A.M., 1998. Dike ascent in partially molten rock. *J. Geophys. Res.* 103, 20901–20919.
- Rushmer, T., 1995. An experimental deformation study of partially molten amphibolite: application to low-fraction melt segregation. *J. Geophys. Res.* 100, 15681–15696.
- Rushmer, T., Brown, M., Bergantz, G., 1998. Penrose conference report: processes of crustal differentiation: crust–mantle interactions, melting and granite migration through the crust. *GSA Today* (in press).
- Rutter, E.H., 1997. The influence of deformation on the extraction of crustal melts: a consideration of the role of melt-assisted granular flow. In: Holness, M. (Ed.), *Deformation-Enhanced Melt Segregation and Metamorphic Fluid Transport*. The Mineralogical Society Series 8, Chapman and Hall, London, pp. 82–110.
- Rutter, E., Neumann, D., 1995. Experimental deformation of partially molten Westerly granite under fluid-absent conditions, with implications for the extraction of granitic magmas. *J. Geophys. Res.* 100 (15), 697–715.
- Saffman, P.G., Taylor, G., 1958. The penetration of a fluid into a porous medium or Hele-Shaw cell containing a more viscous liquid. *Proc. R. Soc. London A* 245, 312–329.
- Sawyer, E.W., 1994. Melt segregation in the continental crust. *Geology* 22, 1019–1022.
- Sawyer, E.W., 1996. Melt–segregation and magma flow in migmatites: Implications for the generation of granite magmas. *Trans. R. Soc. Edinburgh: Earth Sci.* 87, 85–94.
- Sawyer, E.W., 1998. Formation and evolution of granite magmas during crustal reworking: the significance of diatexites. *J. Petrol.* 39, 1147–1167.
- Sawyer, E.W., 1999. Criteria for the recognition of partial melting. *Phys. Chem. Earth (A)* 24, 269–279.
- Skarmeta, J.J., Castelli, J.C., 1997. Intrusión sintectónica del Granito de las Torres del Paine, Andes Patagónicos de Chile. *Rev. Geol. Chile* 24, 55–74.
- Sleep, N.H., 1988. Tapping of melt by veins and dikes. *J. Geophys. Res.* 93, 10255–10272.
- Smith, H.A., Barreiro, B., 1990. Monazite U–Pb dating of staurolite grade metamorphism in pelitic schists. *Contrib. Mineral. Petrol.* 105, 602–615.
- Solar, G.S., 1996. Relationship between ductile deformation and granite magma transfer, Tumbledown Mountain area, west-central Maine. In: van Baalen, M.R. (Ed.), *Guidebook to Field Trips in Northern New Hampshire and Adjacent Regions of Maine and Vermont*, New England Intercollegiate Geological Conference 88, pp. 341–362.
- Solar, G.S., Brown, M., 1999a. The classic high-*T*–low-*P* metamorphism of west-central Maine, USA: is it post-tectonic or syn-tectonic? Evidence from porphyroblast–matrix relations. *Can. Mineral.* 37, 311–333.
- Solar, G.S., Brown, M., 1999b. Contrasting patterns of strain and kinematic partitioning of flow during oblique contraction in the Central Maine belt, Northern Appalachian orogen, USA. *J. Struct. Geol.* (in press).
- Solar, G.S., Pressley, R.A., Brown, M., Tucker, R.D., 1998. Granite ascent in convergent orogenic belts: testing a model. *Geology* 26, 711–714.
- Stevenson, D.J., Scott, D.R., 1987. Melt migration in deformable media. In: Loper, D.E. (Ed.), *Structure and Dynamics of Partially Solidified Systems*. Nijhoff, Dordrecht, pp. 403–415.
- Stewart, D.B., 1989. Crustal processes in Maine. *Am. Mineral.* 74, 698–714.
- Swanson, M.T., 1992. Late Acadian–Alleghenian transpressional deformation: evidence from asymmetric boudinage in the Casco Bay area, coastal Maine. *J. Struct. Geol.* 14, 323–341.
- Talbot, C.J., Rönnlund, P., Schmeling, H., Koyi, H., Jackson, M.P.A., 1991. Diapiric spoke patterns. *Tectonophysics* 188, 187–201.
- Thompson, A.B., 1996. Fertility of crustal rocks during anatexis. *Trans. R. Soc. Edinburgh: Earth Sci.* 87, 1–10.
- Thompson, A.B., Tracy, R.J., 1979. Model systems for anatexis of pelitic rocks. *Contrib. Mineral. Petrol.* 70, 429–438.
- Thompson, A.B., Schulmann, K., Jezek, J., 1997. Thermal evolution and exhumation in obliquely convergent (transpressive) orogens. *Tectonophysics* 280, 171–184.
- Tikoff, B., Teyssier, C., 1992. Crustal-scale, en echelon ‘P-shear’ tensional bridges: a possible solution to the batholithic room problem. *Geology* 20, 927–930.
- Unger, J.D., Liberty, L.M., Phillips, J.D., Wright, B.E., 1989. Creating a 3-dimensional transect of the earth’s crust from craton to ocean basin across the N. Appalachian Orogen. In: Raper, J. (Ed.), *3-Dimensional Applications in Geographical Information Systems*. Taylor and Francis, London, pp. 137–148.
- Van der Pluijm, B.A., van Staal, C.R., 1988. Characteristics and evolution of the Central Mobile Belt, Canadian Appalachians. *J. Geol.* 96, 535–547.
- Van Staal, C.R., de Roo, J.A., 1995. Mid-Paleozoic tectonic evolution of the Appalachian Central Mobile Belt in northern New Brunswick, Canada: collision, extensional collapse and dextral transpression. In: Hibbard, J.P., van Staal, C.R., Cawood, P.A. (Eds.), *Current Perspectives in the Appalachian–Caledonian Orogen*. *Geol. Assoc. Can. Spec. Pap.* 41, 367–389.
- Van Staal, C.R., Dewey, J.F., MacNiocail, C., McKerrow, W.S., 1998. The Cambrian–Silurian tectonic evolution of the northern Appalachians and British Caledonides: history of a complex, west and southwest Pacific-type segment of Iapetus.

- In: Blundell, D.J., Scott, A.C. (Eds.), *Lyell: the Past is the Key to the Present*. Geol. Soc. Spec. Publ. 143, 199–142.
- Vanderhaeghe, O., 1999. Pervasive melt migration from migmatites to leucogranite in the Shuswap Metamorphic Core Complex, Canada: control of regional deformation. *Tectonophysics* 312, 35–55.
- Vidal, P., Cocherie, A., Le Fort, P., 1982. Geochemical investigations of the origin of the Manaslu leucogranite (Himalaya, Nepal). *Geochim. Cosmochim. Acta* 46, 2279–2292.
- Vielzeuf, D., Montel, J.M., 1994. Partial melting of meta-greywackes, Part I. Fluid-absent experiments and phase relationships. *Contrib. Mineral. Petrol.* 117, 375–393.
- Vigneresse, J.L., 1988. Formes et volume des plutons granitiques. *Bull. Soc. Geol. Fr.* 8, 897–906.
- Vigneresse, J.L., 1990. Use and misuse of geophysical data to determine the shape at depth of granitic intrusions. *Geol. J.* 25, 249–260.
- Vigneresse, J.L., 1995a. Control of granite emplacement by regional deformation. *Tectonophysics* 249, 173–186.
- Vigneresse, J.L., 1995b. Crustal regime of deformation and ascent of granitic magmas. *Tectonophysics* 249, 187–202.
- Weinberg, R.F., 1996. The ascent mechanism of felsic magmas: news and views. *Trans. R. Soc. Edinburgh: Earth Sci.* 87, 95–103.
- Weinberg, R.F., 1999. Pervasive felsic magma migration: alternatives to diking? *Lithos* 41, 393–410.
- Weinberg, R.F., Podladchikov, Y., 1994. Diapiric ascent of magmas through power-law crust and mantle. *J. Geophys. Res.* 99, 9543–9559.
- Weinberg, R.F., Podladchikov, Yu.Yu., 1995. The rise of solid diapirs. *J. Struct. Geol.* 17, 1183–1195.
- Weinberg, R.F., Searle, M.P., 1998. The Pangong Injection Complex, Indian Karakoram: a case of pervasive granite flow through hot viscous crust. *J. Geol. Soc., London* 155, 883–891.
- West, D.P. Jr., 1999. Timing of displacements along the Norumbega fault system, south-central and south-coastal Maine. In: Ludman, A., West, D.P. Jr. (Eds.), *Norumbega Fault System of the Northern Appalachians*. Geol. Soc. Am. Spec. Pap. 331, in press.
- West Jr., D.P., Hubbard, M.S., 1997. Progressive localization of deformation during exhumation of a major strike-slip shear zone: Norumbega fault zone, south-central Maine, USA. *Tectonophysics* 273, 185–201.
- Whitehead, J.A., Helfrich, K.R., 1991. Instability of flow with temperature-dependent viscosity: A model of magma dynamics. *J. Geophys. Res.* 96, 4145–4155.
- Wickham, S.M., 1987. The segregation and emplacement of granitic magmas. *J. Geol. Soc., London* 144, 281–297.
- Williamson, K., Seaman, S.J., 1996. K-feldspar megacryst, magma mingling, and granitic magma evolution in the Lexington Batholith, west-central Maine. *Geol. Soc. Am., Abstr. Progr.* 28, A-481.
- Zhu, H., Ebel, J.E., 1994. Tomographic inversion for the seismic velocity structure beneath northern New England using seismic refraction data. *J. Geophys. Res.* 99, 15331–15357.